EXPERIMENTAL TECHNIQUES AND METHODS OF ANALYSIS USED IN SUBMERGED BODY RESEARCH

Alex Goodman
David Taylor Model Basin

This paper deals with the various experimental techniques and methods of analysis which are either presently being used or are contemplated in the near future at the David Taylor Model Basin in the field of dynamic stability and control of submerged bodies. The advantages and disadvantages of the various techniques are discussed. Primary emphasis is placed on the principles and operation of the DTMB Planar-Motion-Mechanism System, since this device is unique and is being used extensively to provide stability and control data for submerged bodies in six degrees of freedom. Emphasis is also placed on the concepts, techniques, and philosophies used in simulator studies and motion analyses. A brief description of the new rotating arm facility, and the free-running model technique are also presented.

NOTATION

The nomenclature defined in DTMB Report 1319 is used herein where applicable. The positive direction of axes, angles, forces, moments, and velocities are shown in the accompanying sketch. The coefficients and symbols are defined as follows:*

Symbol	Dimensionless Form	Definition
A_b	$A_b' = \dfrac{A_b}{l^2}$	Projected area of bow planes
A_r	$A_r' = \dfrac{A_r}{l^2}$	Projected area of rudders
A_s	$A_s' = \dfrac{A_s}{l^2}$	Projected area of stern planes
AP		After perpendicular
AR		Aspect ratio

*All derivatives with respect to angular quantities are given as "per radian."

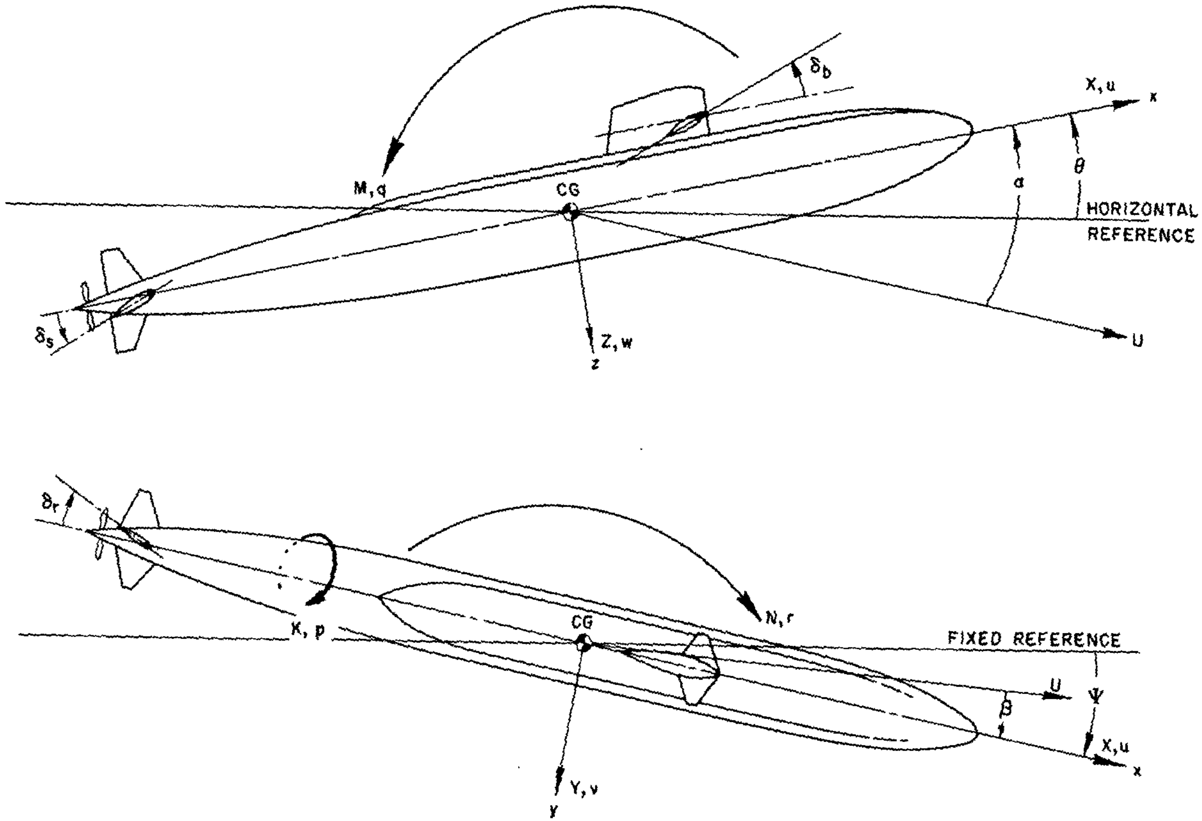
δb
X, u
x
θ
α
HORIZONTAL
REFERENCE
M, q
CG
Z, w
z
U
δs
δr
K, p
N, r
CG
FIXED REFERENCE
U
Ψ
β
X, u
x
Y, v
y

Symbol	Dimensionless Form	Definition
B	$B' = \dfrac{B}{\frac{1}{2}\rho l^2 U^2}$	Buoyancy force
CB		Center of buoyancy of submarine
CG		Center of mass of submarine
c		Damping constant
c_c		Critical damping constant
d	$d' = \dfrac{d}{l}$	Diameter of body
FP		Forward perpendicular
h		Depth of submergence to center of mass
I_x, I_y, I_z	$I_x' = \dfrac{I_x}{\frac{1}{2}\rho l^5}$	Moment of inertia of the body about x-, y-, z-axis
K	$K' = \dfrac{K}{\frac{1}{2}\rho l^3 U^2}$	Hydrodynamic moment about x-axis through center of gravity
K_p	$K_p' = \dfrac{K_p}{\frac{1}{2}\rho l^4 U}$	Derivative of moment component with respect to angular velocity component p
$K_{\dot{p}}$	$K_{\dot{p}}' = \dfrac{K_{\dot{p}}}{\frac{1}{2}\rho l^5}$	Derivative of moment component with respect to angular acceleration component $\dot{p}$
K_r	$K_r' = \dfrac{K_r}{\frac{1}{2}\rho l^4 U}$	Derivative of moment component with respect to angular velocity component r
$K_{\dot{r}}$	$K_{\dot{r}}' = \dfrac{K_{\dot{r}}}{\frac{1}{2}\rho l^5}$	Derivative of moment component with respect to angular acceleration component $\dot{r}$
K_v	$K_v' = \dfrac{K_v}{\frac{1}{2}\rho l^3 U}$	Derivative of moment component with respect to velocity component v

646551 O—62——26

Symbol	Dimensionless Form	Definition
$K_{\dot{v}}$	$K_{\dot{v}}' = \dfrac{K_{\dot{v}}}{\frac{1}{2}\rho l^4}$	Derivative of moment component with respect to acceleration component $\dot{v}$
K_{δ_r}	$K_{\delta_r}' = \dfrac{K_{\delta_r}}{\frac{1}{2}\rho l^3 U^2}$	Derivative of moment component with respect to rudder angle component δ_r
k_y	$k_y' = \dfrac{k_y}{l}$	Radius of gyration of ship and added mass of ship about y-axis
l	$l' = 1$	Characteristic length of submarine
M	$M' = \dfrac{M}{\frac{1}{2}\rho l^3 U^2}$	Hydrodynamic moment about y-axis through center of gravity
M_q	$M_q' = \dfrac{M_q}{\frac{1}{2}\rho l^4 U}$	Derivative of moment component with respect to angular velocity component q
$M_{\dot{q}}$	$M_{\dot{q}}' = \dfrac{M_{\dot{q}}}{\frac{1}{2}\rho l^5}$	Derivative of moment component with respect to angular acceleration component $\dot{q}$
M_w	$M_w' = \dfrac{M_w}{\frac{1}{2}\rho l^3 U}$	Derivative of moment component with respect to velocity component w
$M_{\dot{w}}$	$M_{\dot{w}}' = \dfrac{M_{\dot{w}}}{\frac{1}{2}\rho l^4}$	Derivative of moment component with respect to acceleration component $\dot{w}$
M_δ, N_δ	$M_\delta' = \dfrac{M_\delta}{\frac{1}{2}\rho l^3 U^2}$	Derivative of moment component with respect to control surface angle component δ
M_{δ_b}	$M_{\delta_b}' = \dfrac{M_{\delta_b}}{\frac{1}{2}\rho l^3 U^2}$	Derivative of moment component with respect to bow plane angle component δ_b
M_{δ_s}	$M_{\delta_s}' = \dfrac{M_{\delta_s}}{\frac{1}{2}\rho l^3 U^2}$	Derivative of moment component with respect to stern plane angle component δ_s

Symbol	Dimensionless Form	Definition
M_θ	$M_\theta' = \dfrac{M_\theta}{\frac{1}{2}\rho l^3 U^2}$	Derivative of moment component with respect to pitch angle component θ
M_*	$M_*' = \dfrac{M_*}{\frac{1}{2}\rho l^3 U^2}$	Hydrodynamic moment at zero angle of attack
m	$m' = \dfrac{m}{\frac{1}{2}\rho l^3}$	Mass of submarine, including water in free-flooding spaces
N	$N' = \dfrac{N}{\frac{1}{2}\rho l^3 U^2}$	Hydrodynamic moment about z-axis through center of gravity
N_r	$N_r' = \dfrac{N_r}{\frac{1}{2}\rho l^4 U}$	Derivative of moment component with respect to angular velocity component r
$N_{\dot{r}}$	$N_{\dot{r}}' = \dfrac{N_{\dot{r}}}{\frac{1}{2}\rho l^5}$	Derivative of moment component with respect to angular acceleration component $\dot{r}$
N_v	$N_v' = \dfrac{N_v}{\frac{1}{2}\rho l\ U}$	Derivative of moment component with respect to velocity component v
$N_{\dot{v}}$	$N_{\dot{v}}' = \dfrac{N_{\dot{v}}}{\frac{1}{2}\rho l^4}$	Derivative of moment component with respect to acceleration component $\dot{v}$
N_{δ_r}	$N_{\delta_r}' = \dfrac{N_{\delta_r}}{\frac{1}{2}\rho l^3 U^2}$	Derivative of moment with respect to rudder angle component δ_r
p	$p' = \dfrac{pl}{U}$	Angular velocity component relative to x-axis
$\dot{p}$	$\dot{p}' = \dfrac{\dot{p}l^2}{U^2}$	Angular acceleration component relative to x-axis
q	$q' = \dfrac{ql}{U}$	Angular velocity component relative to y-axis

Symbol	Dimensionless Form	Definition
$\dot{q}$	$\dot{q}' = \dfrac{\dot{q}l^2}{U^2}$	Angular acceleration component relative to y-axis
r	$r' = \dfrac{rl}{U}$	Angular velocity component relative to z-axis
$\dot{r}$	$\dot{r}' = \dfrac{\dot{r}l^2}{U^2}$	Angular acceleration component relative to z-axis
$t_{1/2}$		Time for oscillatory motion to damp to one-half initial amplitude
U	$U' = 1$	Velocity of origin of body axes relative to fluid in feet per second
V_k		Velocity of origin of body axes relative to fluid in knots
v	$v' = \dfrac{v}{U}$	Component along y-axis of velocity of origin of body relative to fluid
$\dot{v}$	$\dot{v}' = \dfrac{\dot{v}l}{U^2}$	Component along y-axis of acceleration of origin of body relative to fluid
w	$w' = \dfrac{w}{U}$	Component along z-axis of velocity of origin of body axes relative to fluid
$\dot{w}$	$\dot{w}' = \dfrac{\dot{w}l}{U^2}$	Component along z-axis of acceleration of origin of body axes relative to fluid
X	$X' = \dfrac{X}{\frac{1}{2}\rho l^2 U^2}$	Hydrodynamic longitudinal force, positive forward
x		The longitudinal axis, directed from the after to the forward end of the submarine with origin taken at the center of gravity
x_B, z_B	$x_B' = \dfrac{x_B}{l}$ $z_B' = \dfrac{z_B}{l}$	Coordinates of center of buoyancy with respect to body axes
x_{CG}	$x_{CG}' = \dfrac{x_{CG}}{l}$	Distance from reference point to center of gravity of model.

Symbol	Dimensionless Form	Definition
Y	$Y' = \dfrac{Y}{\frac{1}{2}\rho l^2 U^2}$	Hydrodynamic lateral force, positive to starboard
Y_r	$Y_r' = \dfrac{Y_r}{\frac{1}{2}\rho l^3 U}$	Derivative of lateral force component with respect to angular velocity component r
$Y_{\dot r}$	$Y_{\dot r}' = \dfrac{Y_{\dot r}}{\frac{1}{2}\rho l^4}$	Derivative of lateral force component with respect to angular acceleration component $\dot r$
Y_v	$Y_v' = \dfrac{Y_v}{\frac{1}{2}\rho l^2 U}$	Derivative of lateral force component with respect to velocity component v
$Y_{\dot v}$	$Y_{\dot v}' = \dfrac{Y_{\dot v}}{\frac{1}{2}\rho l^3}$	Derivative of lateral force component with respect to acceleration component $\dot v$
Y_δ, Z_δ	$Y_\delta' = \dfrac{Y_\delta}{\frac{1}{2}\rho l^2 U^2}$	Derivative of force component with respect to control surface angle component δ
Y_{δ_r}	$Y_{\delta_r}' = \dfrac{Y_{\delta_r}}{\frac{1}{2}\rho l^2 U^2}$	Derivative of lateral force component with respect to rudder angle component δ_r
y		Distance along the transverse axis, directed to starboard with origin taken at center of gravity
Z	$Z' = \dfrac{Z}{\frac{1}{2}\rho l^2 U^2}$	Hydrodynamic normal force, positive downward
Z_q	$Z_q' = \dfrac{Z_q}{\frac{1}{2}\rho l^3 U}$	Derivative of normal force component with respect to angular velocity component q
$Z_{\dot q}$	$Z_{\dot q}' = \dfrac{Z_{\dot q}}{\frac{1}{2}\rho l^4}$	Derivative of normal force component with respect to angular acceleration component $\dot q$
Z_w	$Z_w' = \dfrac{Z_w}{\frac{1}{2}\rho l^2 U}$	Derivative of normal force component with respect to velocity component w

Symbol	Dimensionless Form	Definition
$Z_{\dot{w}}$	$Z_{\dot{w}}' = \dfrac{Z_{\dot{w}}}{\frac{1}{2}\rho l^3}$	Derivative of normal force component with respect to acceleration component $\dot{w}$
Z_{δ_b}	$Z_{\delta_b}' = \dfrac{Z_{\delta_b}}{\frac{1}{2}\rho l^2 U^2}$	Derivative of normal force component with respect to bow plane angle δ_b
Z_{δ_s}	$Z_{\delta_s}' = \dfrac{Z_{\delta_s}}{\frac{1}{2}\rho l^2 U^2}$	Derivative of normal force component with respect to stern-plane angle component δ_s
Z_*	$Z_*' = \dfrac{Z_*}{\frac{1}{2}\rho l^2 U^2}$	Normal force at zero angle of attack
z		Distance along the normal axis, directed from top to bottom (deck to keel), with origin taken at center of gravity
α		The angle of attack; the angle to the longitudinal body axis from the projection into the principal plane of symmetry of the velocity of the origin of the body axes relative to the fluid, positive in positive sense of rotation about the y-axis
β		The drift or sideslip angle; the angle to the principal plane of symmetry from the velocity of the origin of the body axes relative to the fluid, positive in the positive sense of rotation about the z-axis
δ		Angular displacement of a control surface
δ_b		Angular displacement of bow planes, positive trailing edge down
δ_r		Angular displacement of rudders, positive trailing edge port
δ_s		Angular displacement of stern planes, positive trailing edge down
θ		The angle of pitch; the angle of elevation of the x-axis positive bow up
ρ	$\rho' = 1$	Mass density of water
σ_i	$\sigma_i' = \sigma_i \dfrac{l}{U}$	Roots of stability equation, $i = 1, 2, \ldots$

Symbol	Dimensionless Form	Definition
ψ		The angle of yaw
ω	$\omega' = \frac{\omega l}{U}$	Circular frequency of oscillation
ω_n	$\omega_n' = \frac{\omega_n l}{U}$	Natural frequency of undamped oscillation

Subscripts:

in	In-phase component of force or moment
out	Out-of-phase or quadrature component of force or moment
o	Maximum amplitude
1	Associated with forward strut
2	Associated with aft strut
m	Model.

INTRODUCTION

The problems associated with the dynamic behavior of the submarine and other submerged bodies, that is, stability, performance, and ease of handling, have become increasingly more and more important with each new increase in submerged speed. This has been particularly true for motions in the vertical plane since the submarine must be operated, strictly on instruments, within the confines of a layer of water usually no greater than a few boat lengths. Also, the increase in submerged speed has given rise to some serious dynamic problems for motions in the horizontal plane and made the problem of emergency recovery increasingly more acute.

In the early stages of development in the field of submarine stability and control the designer was faced with the problem of providing a combination of characteristics and means for controlling the submarine which would result in satisfactory dynamic behavior. A major difficulty in providing for this was the lack of sufficient information to guide him in the choice of a combination of physical characteristics which would result in adequate stability, performance, and ease of handling. Another major difficulty was the lack of straightforward design methods and experimental or theoretical techniques for obtaining a desired combination of characteristics. In those cases where the results of model tests in the form of the various hydrodynamic coefficients were available, the interpretations that could readily be made relating them to adequate dynamic behavior were rather limited. The designer was further handicapped in that he had no standards by which he could evaluate the dynamic behavior of the submarine.

The mission of the Stability and Control Division at the David Taylor Model Basin has been, therefore, to remedy this situation. This has been partially accomplished by the development of a set of desirable handling qualities which could be used in optimizing the submerged body design [1], development of methods which give an objective evaluation of the submerged body's dynamic behavior, and improvements in, and development of, new prediction and experimental techniques which could be used by the designer to evaluate the submerged body performance.

This paper presents and describes the various experimental techniques and methods of analysis used at the David Taylor Model Basin in the field of dynamic stability and control of submerged bodies. The advantages and disadvantages of the various techniques are presented. Primary emphasis is placed on the principles and operation of the DTMB Planar-Motion-Mechanism System [2] as well as on the concepts, techniques, and philosophies used in simulator and motion analysis studies. Throughout the presentation, it will be noted that frequent references will be made to the use of the various techniques as applied to the submarine stability and control problem. Most of the data acquired by these techniques have been for submarines because of the urgency that submarine problems have assumed in recent years. It should be noted, however, that these techniques are also applicable to other types of marine vehicles.

COMPARISON OF EXPERIMENTAL TECHNIQUES

The various approaches to the solution of problems in the field of dynamic stability and control of a submerged body moving through a fluid, shown in Fig. 1, have been employed by naval architects and aerodynamicists for many years. Many investigators have used the free-running or flying-model techniques since a direct evaluation of the performance of the design is provided [3,4]. However, this method does not provide data which can be related to the physical characteristics of the design or to support the design changes required for improved performance. The full-scale technique suffers from the same shortcomings. However, this technique is used mainly for providing data for model-full-scale correlation.

In recent years, the development of general-purpose analog and high-speed digital computers has resulted in the extensive use of the mathematical-model technique. This technique, which is based on a thorough analysis of the differential equations which govern the motions, provides a solution and basic understanding of the dynamic stability and control problems of a submerged body. However, these differential equations of motion are comprised of numerous coefficients or derivatives which are of hydrodynamic origin.

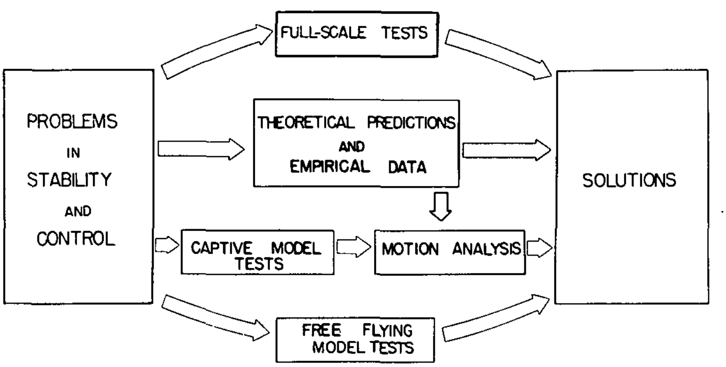

Fig. 1. Approaches to problems in stability and control

Consequently, to obtain solutions for any given configuration by means of this technique, it is necessary to know these coefficients with reasonable accuracy. Many attempts have been made in the past to fulfill this requirement by utilizing various experimental (captive model) and theoretical techniques, or combinations of both.

Among the various captive-model techniques used, fairly refined methods have been developed by model basins and wind tunnels for measuring forces and moments due to body orientation and control deflection; the so-called static stability and control coefficients. However, the various experimental methods used to determine forces and moments associated with variations in linear acceleration, angular velocity, and angular acceleration have been successful in only a limited number of cases. The techniques that have been tried in this respect have required the use of facilities such as the rotating arm, free oscillator, forced oscillator, curved-flow and rolling-flow tunnels, and curved models in a straight flow facility [3]. Each of these techniques has certain limitations and problems associated with either accuracy of instrumentation, model support, friction, accuracy of flow (curved and rolling flow) [5,6], and accuracy of model construction (curved model). Also, none of these techniques provide a direct measure of all the hydrodynamic coefficients required in the equations of motion for six degrees of freedom. The DTMB Planar-Motion-Mechanism System recently developed at the David Taylor Model Basin, however, incorporates in one device a means for experimentally determining all of the hydrodynamic-stability coefficients required in the equations of motion for a submerged body in six degrees of freedom.

A comparison of the main advantages and disadvantages of several of the basic experimental techniques that have been discussed is presented in Table 1. Based on this comparison, it can be seen that the mathematical model technique, in conjunction with accurately determined hydrodynamic coefficients, provides the most powerful and versatile design and research tool for the study and analysis of stability and control problems.

PLANAR-MOTION-MECHANISM SYSTEM

The DTMB Planar-Motion-Mechanism System incorporates in one device a means for experimentally determining all of the hydrodynamic-stability and control coefficients required in the equations of motion for a submerged body in six degrees of freedom. These include the static-stability and control, rotary-stability, and acceleration coefficients. The unique features of the system are the methods used to impart hydrodynamically pure pitching, heaving, and rolling motions to a given submerged body, as well as the dynamometry and data analysis equipment employed. These enable the explicit and accurate determination of individual derivatives without resort to the solution of simultaneous equations as is necessary when other types of oscillation devices are used. Although the system was designed primarily for submerged body research it can also be used to determine the hydrodynamic coefficients for other types of marine vehicles such as hydrofoil boats and ground effect machines.

General Considerations

The derivatives and composition of the equations of motion have formed the subject of numerous text books and papers [7-9]. For the purpose of this paper, therefore, only the general nature of these equations are considered. This is done to give some insight into the problems which must be faced in the design of experimental facilities for the evaluation of the equations.

Table 1
Comparison of Experimental Techniques

(a) Free-Running Model Technique	
Advantages	
1. Direct evaluation of performance of specific designs 2. Can be economical and expedient	3. Can be used to study extreme maneuvers which may be too complicated to handle by analytical or computer methods
Disadvantages	
1. Does not provide data which can be directly related to the design of body and individual appendages 2. Does not provide data to directly support design changes to effect improvements in performance	3. Froude or dynamic scaling necessary for mass, moment of inertia, and metacentric stability
(b) Mathematical Model Techniques	
Advantages	
1. Provides means of evaluating handling qualities or operational characteristics of proposed design well in advance of construction 2. Provides simple means of studying effects of practical variations of basic design which may be necessary to improve performance 3. Can be used to determine effects of various environmental conditions on performance	4. Provides measures of capabilities of the design tempered by existence of human operator or automatic control device in control loop 5. Can be used in human engineering studies 6. Can be used to study overall performance of various combined systems 7. Can be used to train personnel
Disadvantages	
1. Requires an accurate set of hydrodynamic coefficients of the design for the equations of motion	2. Requires expensive facilities
(c) Captive Model Techniques	
Advantages	
1. Provides basic data on which to support design of individual body and appendages 2. Provides basic data which can be used with the equations of motion in computer and simulator studies to evaluate inherent and closed-loop performance 3. Provides data which can be directly utilized in design of automatic control systems	4. Results can be utilized to study effects of proposed design changes without additional model tests 5. Data are perpetuated so that further studies can be made at a later time without the need for additional model tests 6. Provides powerful tool for doing research or systematic series work on stability and control 7. Dynamic scaling not necessary
Disadvantages	
1. Data are one step removed from directly indicating all the handling qualities 2. Method may become uneconomical for evaluating performance of <u>one</u> specific design	3. Requires expensive facilities

The hydrodynamic forces and moments which enter into the equations of motion as coefficients are usually classified into three categories: static, rotary, and acceleration. The static coefficients are due to components of linear velocity of the body relative to the fluid, the rotary coefficients are due to angular velocity, and the acceleration coefficients are due to either linear or angular acceleration. Within limited ranges the coefficients are linear with respect to the appropriate variables and thus may be utilized as static, rotary, and acceleration derivatives in linearized equations of motion.

It may be concluded from the foregoing classification, that the experimental determination of the coefficients of the equations of motion requires facilities which will impart linear and angular velocities and accelerations to a given body with respect to a fluid. For example, the usual basin facilities have carriages designed to tow models in a straight line at constant speed. Such facilities can be equipped to orient models in either pitch or yaw to obtain the static coefficients. However, more specialized types of facilities, such as rotating arm or oscillator, are required to impart the angular velocities that are necessary to obtain rotary coefficients. The oscillator type of facility provides also linear and angular accelerations so that the acceleration coefficients may be determined experimentally.

The choice of a suitable facility for determining hydrodynamic coefficients involves many considerations pertaining to accuracy, expediency, and ease of data analysis. A detailed treatment of these problems is beyond the scope of this paper. However, of primary concern is the degree to which the experimental technique involves explicit relationships and avoids the need for solutions of matrices. Also techniques which involve extrapolations should be avoided. To illustrate, a carriage which tows a model at uniform velocity in straight-line pitched or yawed flight is a direct and explicit means of determining static coefficients. Similarly, a rotating arm which tows a model at uniform angular velocity and tangential to the circular path at each of several different radii is a means for determining rotary coefficient explicitly. On the other hand, the use of the rotating arm to obtain static coefficients should be considered as an indirect procedure since the data must be extrapolated to infinite radius. The usual oscillator techniques are even more indirect and, at best, require solutions of simultaneous equations to obtain rotary and acceleration derivatives.

Each of the techniques mentioned can be used most advantageously for obtaining one category of hydrodynamic coefficients. The straight-line towing carriage supplies only the static coefficients. The rotating arm supplies rotary coefficients directly and static coefficients indirectly. The oscillator supplies all three categories of coefficients, but all indirectly.

The foregoing considerations suggest the desirability of having a single system to determine explicitly all of the coefficients required in the equations of motion for six degrees of freedom. To accomplish this objective, it is necessary to develop a facility which can move a body through water with "hydrodynamically pure" linear velocities, angular velocities, linear accelerations, and angular accelerations in all degrees of freedom. This concept forms the basis of the DTMB Planar-Motion-Mechanism System.

Principles of Operation

The DTMB Planar-Motion-Mechanism System as it physically exists is described briefly in the next section. It is desirable, however, to consider first the principles underlying the operation of the mechanism so that the design concept can be generally understood. In the interest of simplicity the mode of operation applicable only to submerged bodies in the vertical plane will be used to describe the principles of the system. The system of axes as well as the symbols and coefficients used in this section have been defined in the notation at the beginning of this paper.

The kind of motion for static coefficients is commonly used by wind tunnel and model basin facilities and, therefore, does not need to be explained in detail. Figure 2 schematically represents this type of motion. The components are given with respect to a body-axis system with the origin at the center of gravity, *CG*.

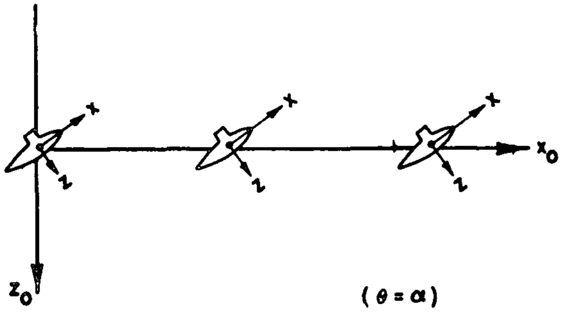

Fig. 2. Straight-line pitched motion for steady-state tests

The system produces this motion by using a towing carriage to tow the model in a straight path at constant velocity. Discrete pitch angles for each run are set by a tilt table which supports the model through a pair of twin struts. Control surface angles are also set discretely for each run. Forces are measured by internal balances at each of the two struts to obtain static forces and moments.

The unique feature of the DTMB Planar Motion Mechanism is the kinds of motions produced to enable the explicit determination of the rotary and acceleration coefficients. Sinusoidal motions are imparted to the model at the point of attachment of each of the two towing struts while the model is being towed through the water by the carriage. The motions are phased in such a manner as to produce the desired conditions of hydrodynamically "pure heaving" and "pure pitching." It is possible also, if required for any reason, to produce various combinations of pitching and heaving. Figure 3 illustrates various types of motions including (a) the type of motion usually associated with oscillators, (b) pure heaving, and (c) pure pitching. The latter two are the basic motions associated with the DTMB Planar Motion Mechanism. The pure rolling motion is not illustrated but consists simply of oscillations about the longitudinal body axis.

The oscillator motion depicted by Fig. 3a is actually a combination of pure pitching and heaving motions. Since the *CG* is constrained to move in a straight path while the model, which oscillates in a see-saw fashion, assumes sinusoidally varying angles of attack and pitch angles. As a result a mixture of static, rotary, and acceleration forces and moments is produced. It becomes necessary, therefore, to perform a similar oscillation about a second reference point. The two oscillation conditions together with the static tests provide data which can be used to separate the hydrodynamic coefficients. The solution of simultaneous equations involved in this process, however, could lead to errors because of the wide differences in magnitude between the various individual coefficients. The oscillator type of

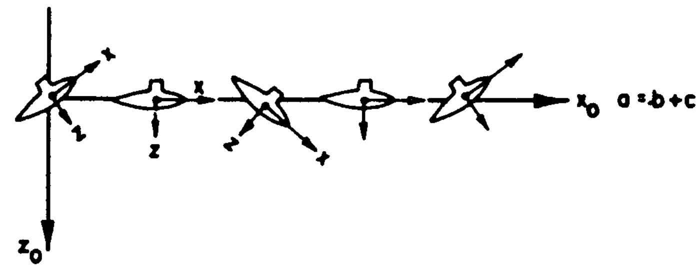

(a) Combined pitching and heaving

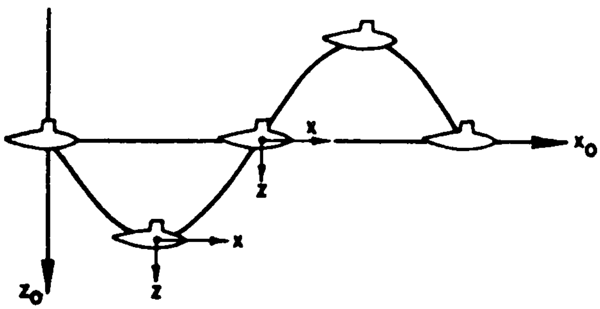

(b) Pure heaving

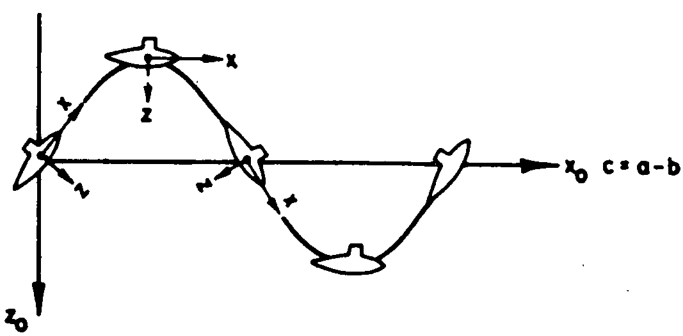

(c) Pure pitching

Fig. 3. Oscillation types of motion

motion is produced by the Planar Motion Mechanism when the two struts move sinusoidally 180 degrees out of phase with each other.

The pure heaving motion shown in Fig. 3b is obtained when both struts move sinusoidally in phase with each other. This results in a motion whereby the model *CG* moves in a sinusoidal path while the pitch angle θ is invariant with time.

The pure pitching motion shown in Fig. 3c is obtained by moving both struts out of phase with each other; the phase angle between struts, ϕ_s, is dependent upon frequency of oscillation, forward speed, and distance of each strut from the *CG*. This relationship can be expressed as

$$\cos \phi_s = \frac{1 - \left(\frac{\omega x}{U}\right)^2}{1 + \left(\frac{\omega x}{U}\right)^2}$$

and is derived as Eq. (A20) in Appendix A. The resulting motion is one in which the model *CG* moves in a sinusoidal path with the model axis always tangent to the path (angle of attack $\alpha = 0$).

The process for obtaining translatory acceleration derivatives from pure heaving tests is represented diagrammatically in Fig. 4. The diagrams across the top of the figure show the motions of the aft and forward struts with respect to each other. Corresponding positions of a component resolver (which has been replaced by a sine-cosine potentiometer in the new system), provided with the electrical system to rectify the sinusoidal signals from the force balances, are also shown. At the left is a column of graphs showing the resulting motions and forces at the *CG*. The right-hand column contains the mathematical relationships represented by each graph. Descending from the top of Fig. 4, there is the vertical displacement z curve, the associated velocity $\dot{z}$ curve, the associated acceleration $\ddot{z}$ curve, and the vertical force Z_R curve. It may be noted that the Z_R curve is displaced in point of time from the z curve by phase angle ϕ. Thus Z_R can be considered as being made up of two components, one in phase with the motion at the *CG*, Z_{in}, and the other in quadrature with the motion at the *CG*, Z_{out}. The shaded area per cycle under each curve represents the magnitudes of Z_{in} and Z_{out}, respectively.

The process for obtaining rotary and angular acceleration derivatives from pure pitching tests is represented diagrammatically in Fig. 5. The order followed is similar to that shown in Fig. 4. In this case, the pitch angle traces (θ, $\dot{\theta}$, and $\ddot{\theta}$) are of primary interest. The Z_R curve is displaced in point of time from the θ curve by phase angle ϕ. The procedure for resolving the resultant force into in-phase and quadrature components is similar to that for the pure heaving case. The shaded area per cycle under each curve represents the magnitudes of Z_{in} and Z_{out}, respectively.

In the pure heaving case the in-phase component of force is directly related to the linear acceleration and, therefore, can be used to compute explicitly the associated acceleration derivatives. Similarly, in the pure pitching case the in-phase component of force is directly related to the angular acceleration and the quadrature component is directly related to the angular acceleration and the quadrature component is directly related to the angular velocity. Thus both the angular acceleration and rotary derivatives can be computed explicitly. The relationships between the various rotary and acceleration derivatives and the respective

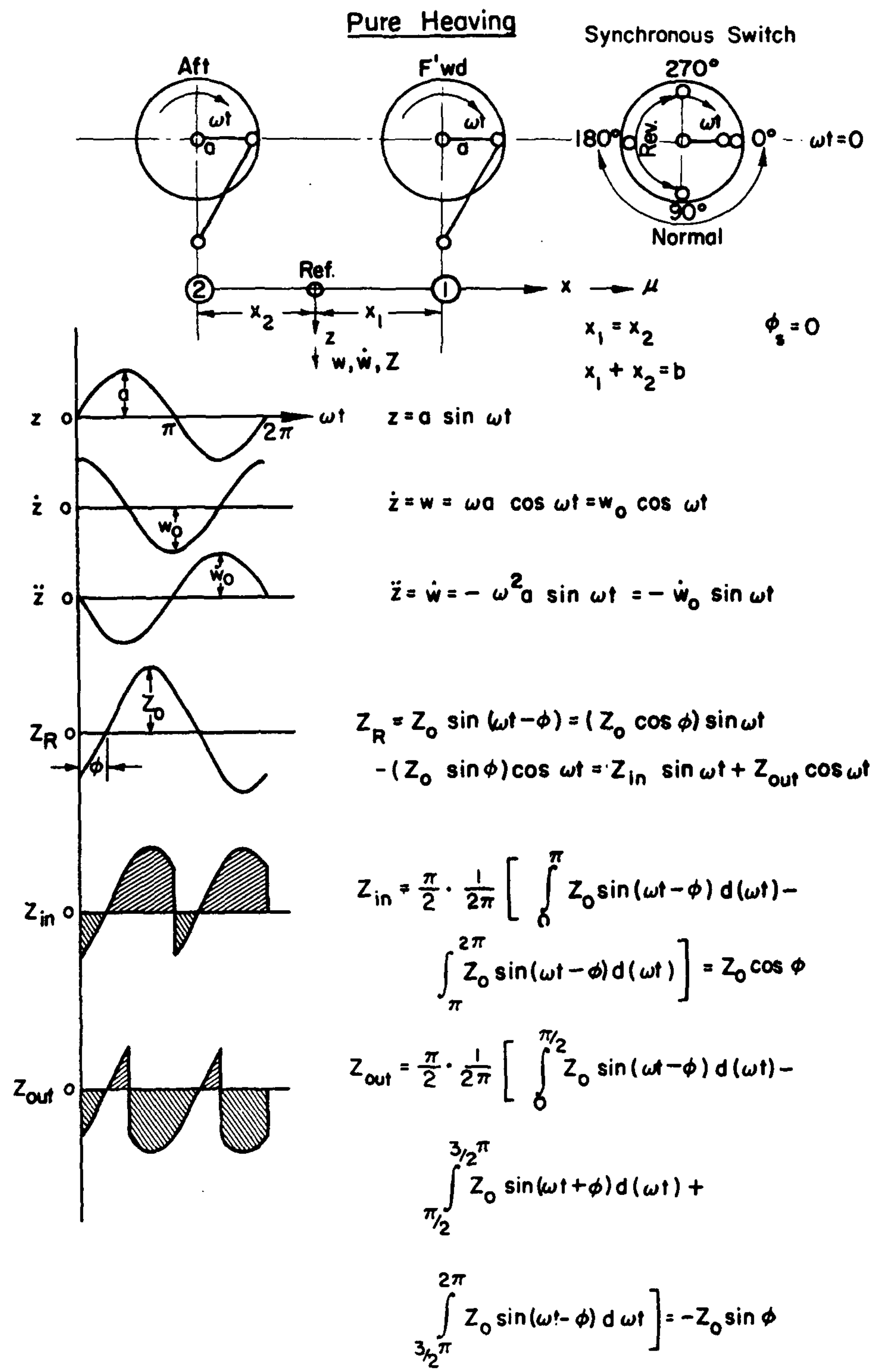

Fig. 4. Analysis of pure heaving motion

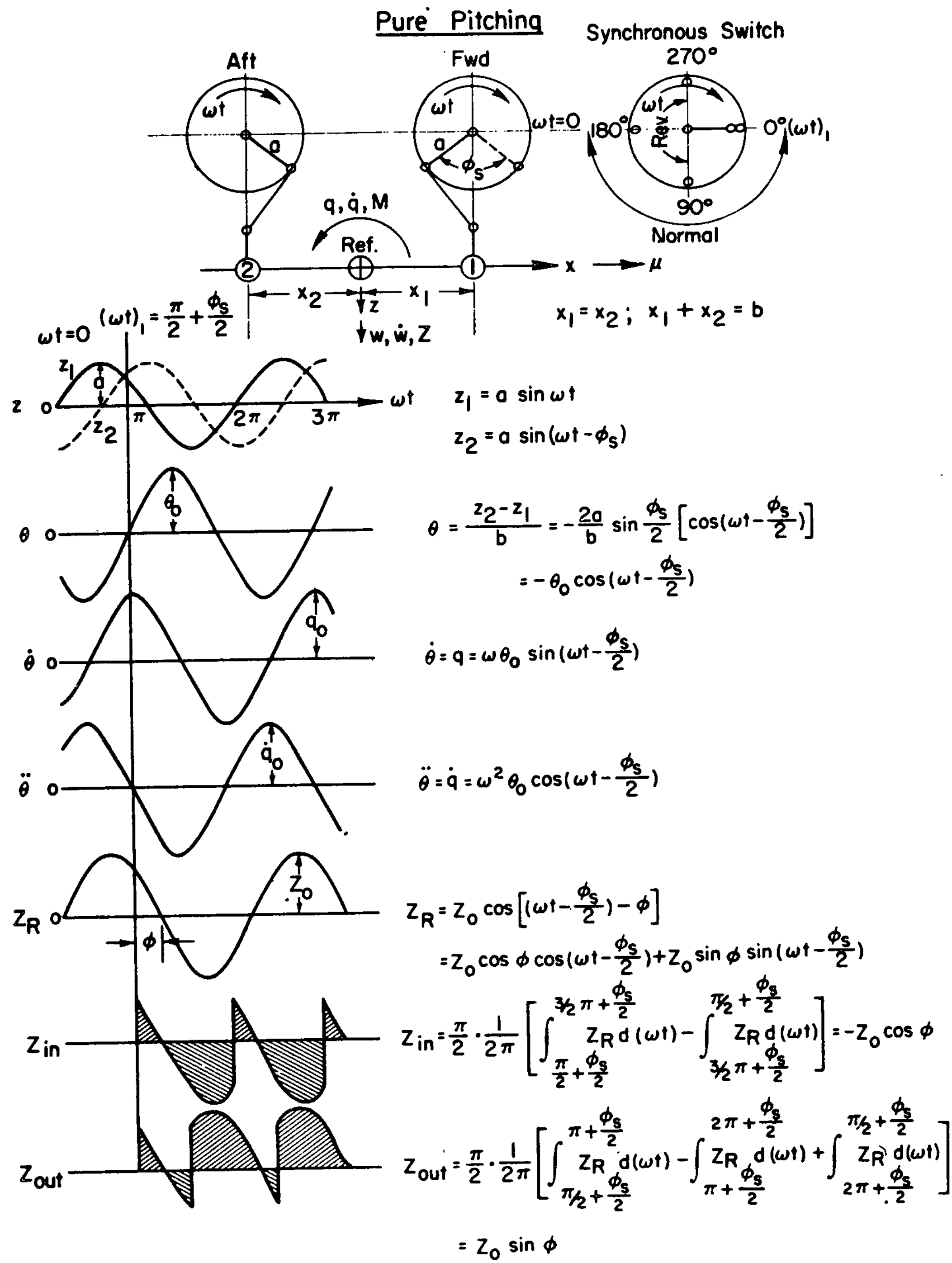

Fig. 5. Analysis of pure pitching motion

in-phase and quadrature components of force are presented in Table 2. The derivation of these reduction equations is presented in Appendix B.

Description of Facility

The DTMB Planar-Motion-Mechanism System is a complete system for obtaining hydrodynamic coefficients from model tests. It embraces all mechanical, electrical, and electronic components necessary to carry out all functions from the delivery of the model to finalized processing of data preparatory to analysis. This includes preparation of the model for testing, conduct of static and oscillation tests, sensing and recording of test data, and processing data digitally in tabulated form. The main features of the system such as model support and positioning equipment, forced-motion mechanism, dynamometry, and Instrumentation Penthouse containing recording and control equipment are shown in Figs. 6 to 23. A description of each of these components has been presented in great detail in Ref. 2. However, the roll-oscillation mechanism and new instrumentation system shown in Figures 15, 20, and 22 were developed and placed into operation after the publication of Ref. 2 and have not been described heretofore.

Roll-Oscillation System – Briefly, the roll-oscillation system produces an oscillation of the body about its longitudinal axes. Modifications and additions to the drive system and roll gage assembly, shown in Figs. 13 and 17, respectively, were required to incorporate this additional mode of motion.

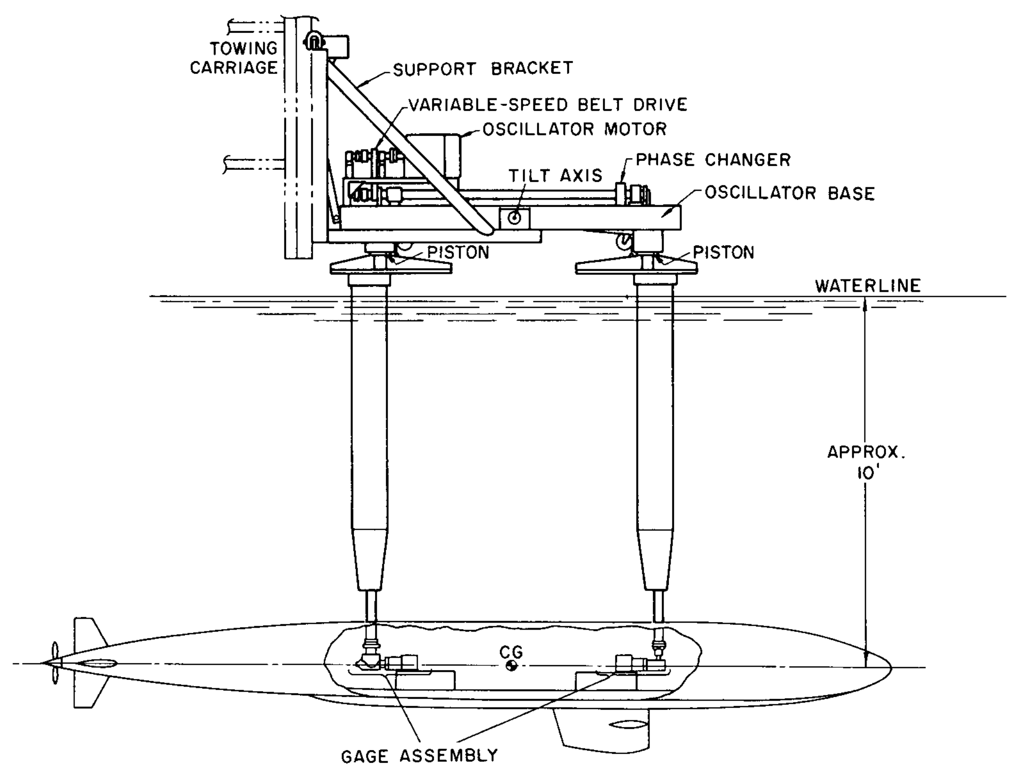

Fig. 6. Schematic arrangement of DTMB Planar Motion Mechanism with model attached

646551 O—62——27

Table 2
Reduction Equations for Rotary and Acceleration Derivatives*

Vertical Plane		
Derivative	**Model Erect**	**Model Inverted**
$Z_{\dot w}' - m_m'$	$-\dfrac{\partial[(Z_1')_{in} + (Z_2')_{in}]}{\partial \dot w_o'}$	$\dfrac{\partial[(Z_1')_{in} + (Z_2')_{in}]}{\partial \dot w_o'}$
$M_{\dot w}' + x_{CG}'m_m'$	$-\dfrac{x}{\ell}\,\dfrac{\partial[(Z_2')_{in} - (Z_1')_{in}]}{\partial \dot w_o'}$	$\dfrac{x}{\ell}\,\dfrac{\partial[(Z_2')_{in} - (Z_1')_{in}]}{\partial \dot w_o'}$
$Z_q' + m_m'$	$\dfrac{\partial[(Z_1')_{out} + (Z_2')_{out}]}{\partial q_o'}$	$-\dfrac{\partial[(Z_1')_{out} + (Z_2')_{out}]}{\partial q_o'}$
$M_q' - x_{CG}'m_m'$	$\dfrac{x}{\ell}\,\dfrac{\partial[(Z_2')_{out} - (Z_1')_{out}]}{\partial q_o'}$	$-\dfrac{x}{\ell}\,\dfrac{\partial[(Z_2')_{out} - (Z_1')_{out}]}{\partial q_o'}$
$Z_{\dot q}' + x_{CG}'m_m'$	$\dfrac{\partial[(Z_1')_{in} + (Z_2')_{in}]}{\partial \dot q_o'}$	$\dfrac{\partial[(Z_1')_{in} + (Z_2')_{in}]}{\partial \dot q_o'}$
$M_{\dot q}' - I_{y_m}'$	$\dfrac{x}{\ell}\,\dfrac{\partial[(Z_2')_{in} - (Z_1')_{in}]}{\partial \dot q_o'} + \dfrac{\dfrac{(M_\theta)_m}{\frac{1}{2}\rho\ell^5}}{\omega^2}$	$-\dfrac{x}{\ell}\,\dfrac{\partial[(Z_2')_{in} - (Z_1')_{in}]}{\partial \dot q_o'} + \dfrac{\dfrac{(M_\theta)_m}{\frac{1}{2}\rho\ell^5}}{\omega^2}$
Horizontal Plane		
Derivative	**Starboard Down**	**Port Down**
$Y_{\dot v}' - m_m'$	$-\dfrac{\partial[(Y_1')_{in} + (Y_2')_{in}]}{\partial \dot v_o'}$	$\dfrac{\partial[(Y_1')_{in} + (Y_2')_{in}]}{\partial \dot v_o'}$
$N_{\dot v}' - x_{CG}'m_m'$	$\dfrac{x}{\ell}\,\dfrac{\partial[(Y_2')_{in} - (Y_1')_{in}]}{\partial \dot v_o'}$	$-\dfrac{x}{\ell}\,\dfrac{\partial[(Y_2')_{in} - (Y_1')_{in}]}{\partial \dot v_o'}$
$Y_r' - m_m'$	$-\dfrac{\partial[(Y_1')_{out} + (Y_2')_{out}]}{\partial r_o'}$	$+\dfrac{\partial[(Y_1')_{out} + (Y_2')_{out}]}{\partial r_o'}$
$N_r' - x_{CG}'m_m'$	$+\dfrac{x}{\ell}\,\dfrac{\partial[(Y_2')_{out} - (Y_1')_{out}]}{\partial r_o'}$	$-\dfrac{x}{\ell}\,\dfrac{\partial[(Y_2')_{out} - (Y_1')_{out}]}{\partial r_o'}$
$Y_{\dot r}' - x_{CG}'m_m'$	$-\dfrac{\partial[(Y_1')_{in} + (Y_2')_{in}]}{\partial \dot r_o'}$	$\dfrac{\partial[(Y_1')_{in} + (Y_2')_{in}]}{\partial \dot r_o'}$
$N_{\dot r}' - I_{z_m}'$	$\dfrac{x}{\ell}\,\dfrac{\partial[(Y_2')_{in} - (Y_1')_{in}]}{\partial \dot r_o'} \quad \dfrac{\dfrac{(N_\psi)_m}{\frac{1}{2}\rho\ell^5}}{\omega^2}$	$-\dfrac{x}{\ell}\,\dfrac{\partial[(Y_2')_{in} - (Y_1')_{in}]}{\partial \dot r_o'} \quad \dfrac{\dfrac{(N_\psi)_m}{\frac{1}{2}\rho\ell^5}}{\omega^2}$
$K_{\dot v}'$	$-\dfrac{\partial(K')_{in}}{\partial \dot v_o'}$	$\dfrac{\partial(K')_{in}}{\partial \dot v_o'}$
K_r'	$-\dfrac{\partial(K')_{out}}{\partial r_o'}$	$+\dfrac{\partial(K')_{out}}{\partial r_o'}$
$K_{\dot r}'$	$-\dfrac{\partial(K')_{in}}{\partial \dot r_o'}$	$\dfrac{\partial(K')_{in}}{\partial \dot r_o'}$
K_p'	$-\dfrac{\partial(K')_{out}}{\partial p_o'}$	$-\dfrac{\partial(K')_{out}}{\partial p_o'}$
$K_{\dot p}' - I_{x_m}'$	$-\dfrac{\partial(K')_{in}}{\partial \dot p_o'} + \dfrac{\dfrac{(K_\phi)_m}{\frac{1}{2}\rho\ell^5}}{\omega^2}$	$-\dfrac{\partial(K')_{in}}{\partial \dot p_o'} + \dfrac{\dfrac{(K_\phi)_m}{\frac{1}{2}\rho\ell^5}}{\omega^2}$
$\dot w_o' = \dfrac{a}{\ell}\,\dfrac{\omega^2\ell^2}{U^2}$	$\dot v_o' = \dfrac{a}{\ell}\,\dfrac{\omega^2\ell^2}{U^2}$	
$q_o' = \dfrac{\omega\ell}{U}\,\dfrac{2a}{b}\sin\dfrac{\phi_s}{2}$	$r_o' = \dfrac{\omega\ell}{U}\,\dfrac{2a}{b}\sin\dfrac{\phi_s}{2}$	$p_o' = \phi_o\dfrac{\omega\ell}{U}$
$\dot q_o' = \dfrac{\omega^2\ell^2}{U^2}\,\dfrac{2a}{b}\sin\dfrac{\phi_s}{2}$	$\dot r_o' = \dfrac{\omega^2\ell^2}{U^2}\,\dfrac{2a}{b}\sin\dfrac{\phi_s}{2}$	$\dot p_o = \phi_o\dfrac{\omega^2\ell^2}{U^2}$

* m_m', $(M_\theta)_m$, $(N_\psi)_m$, and $(K_\phi)_m$ determined from standstill tests

Fig. 7. Tilt table with model attached mounted on storage stand

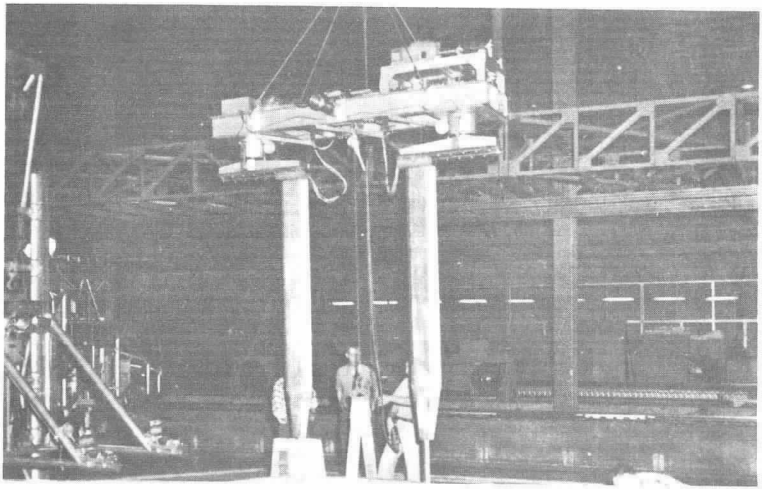

Fig. 8. Tilt table with model attached being moved by overhead crane

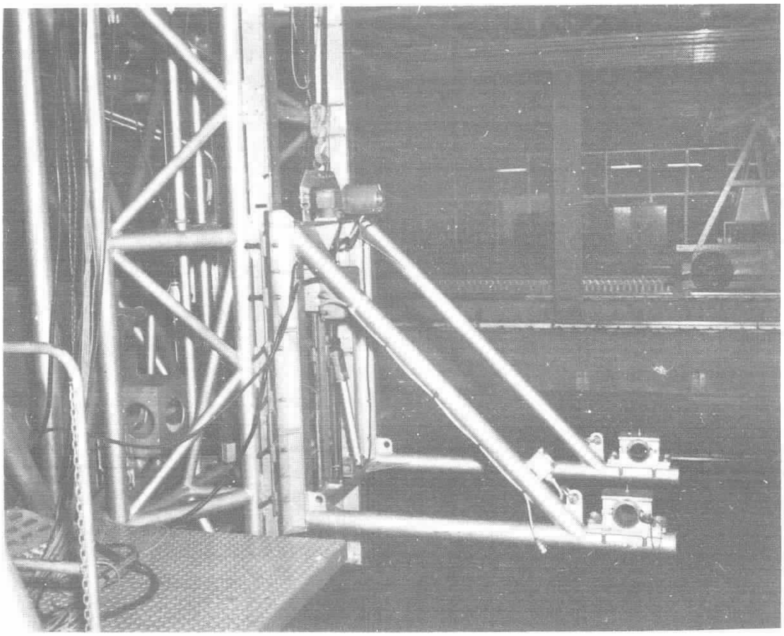

Fig. 9. Tilt table support bracket attached to towing carriage

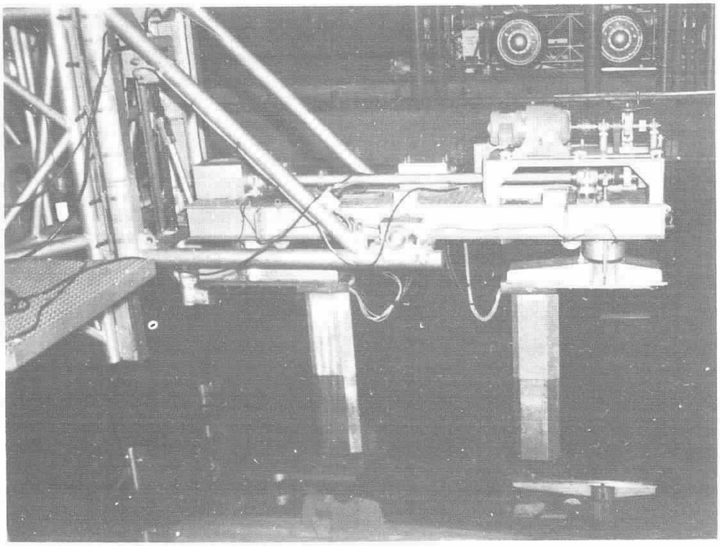

Fig. 10. Tilt table

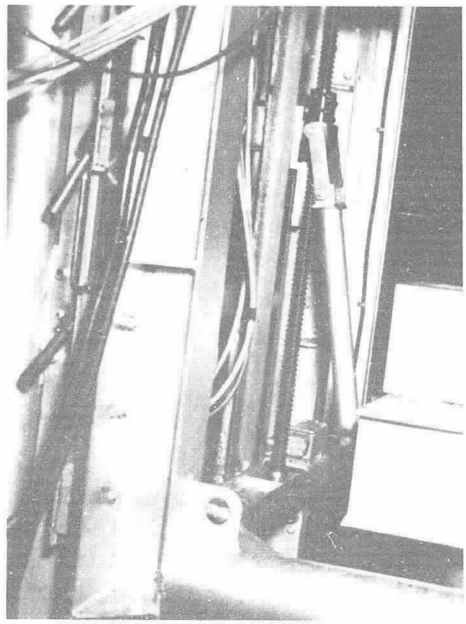

Fig. 11. Tilting mechanism

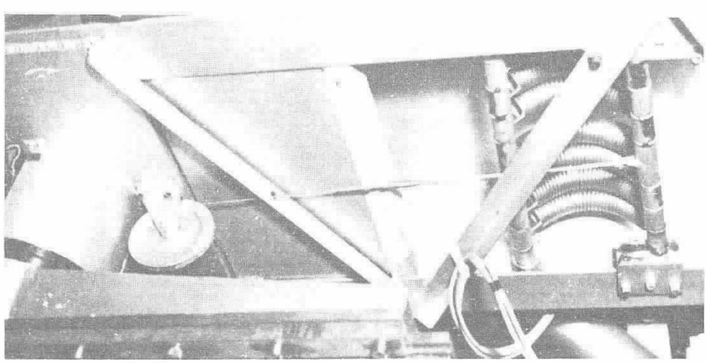

Fig. 12. Counterbalancing device

The lower pulley shaft of the drive system, shown in Fig. 13, was modified so that it would operate in two modes; as a power transmitting shaft for the pure heaving and pitching modes, and as a power transmitting shaft for the rolling mode. This is accomplished by mounting the lower set of Gilmore pulleys on a shaft which is support by ball bearings to an inner shaft which is directly coupled to the main drive shaft. For pitching and heaving, the outer and inner pulley shafts are connected by means of a tapered pin. For the rolling mode, the taper pin is removed, and the strut-pistons are locked. The pulley at the end of the idler shaft, shown in Fig. 15a, is connected by means of a Gilmore belt to a pulley-shaft system attached to the aft strut-piston. This pulley can be positioned along a keyed shaft so that a fixed relationship is maintained between the pulley and the aft strut. Power is transmitted to the slider crank mechanism attached to the aft strut, by means of another

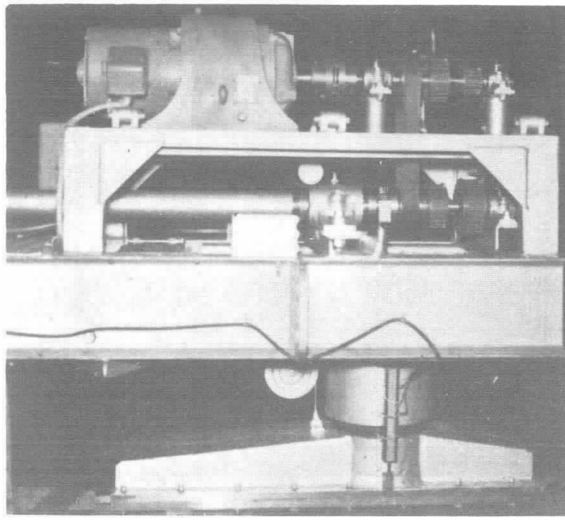

Fig. 13. Drive system for forced-motion mechanism

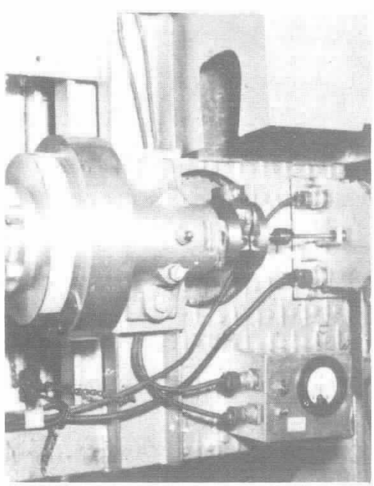

(a) Top view

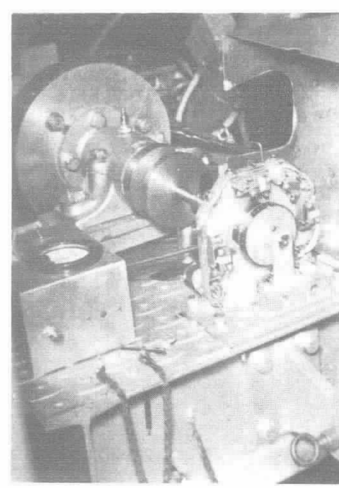

(b) End view

Fig. 14. Phase-changer and synchronous switch

pulley-Gilmore belt system. The slider crank mechanism used in this case has an eccentricity of 0.125 inches and a connecting rod length of 5.000 inches; or a length of connecting rod to eccentricity of 40.0. The sinusoidal motion produced by the slider crank mechanism is transmitted to a 1.0-inch-diameter push-rod, shown in Fig. 15b, which is guided by linear bearings attached to the aft strut. The end of the push-rod is attached to the modified roll gage by means of the 3.000-inch crank arm assembly shown in Fig. 15c. The maximum amplitude of the roll oscillation is therefore, ±2.38 degrees

$$\left(\phi_0 = \tan^{-1} \frac{0.125}{3.000}\right)$$

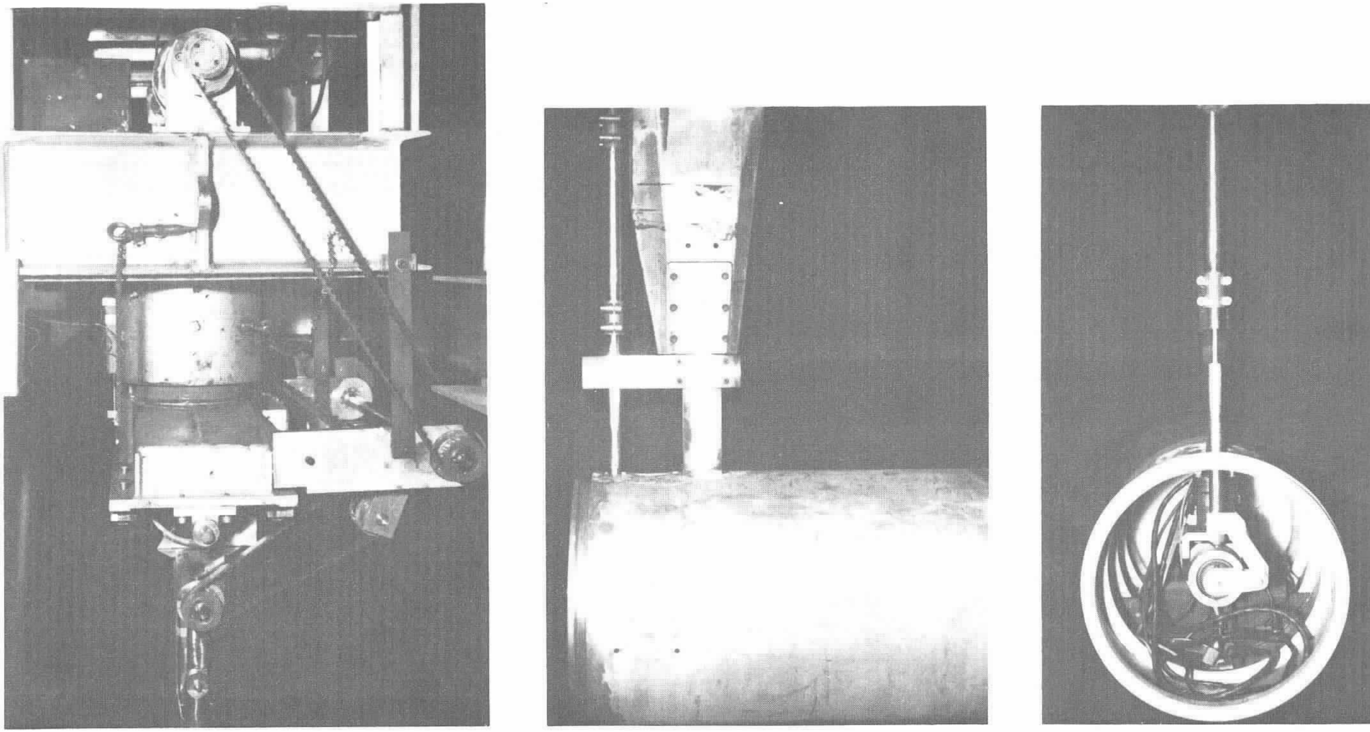

(a) Roll oscillation drive mechanism

(b) Roll push rod

(c) Push-rod attachment to roll balance

Fig. 15. Roll oscillation mechanism

Fig. 16. Modular force gage

(a) Assembled with gimbal

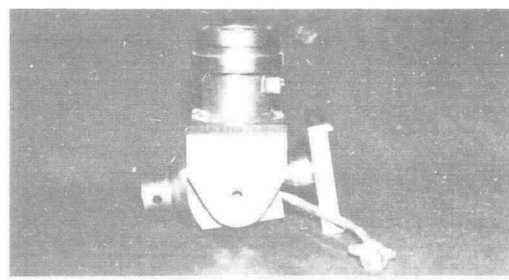

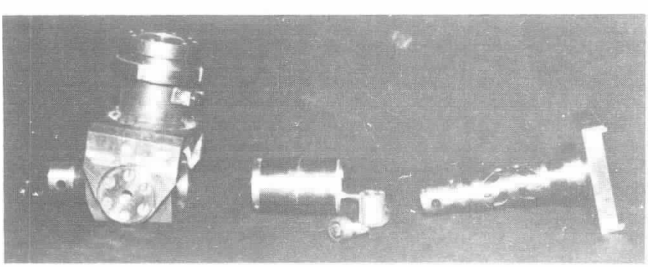

(b) Individual components

(c) Modified roll gage

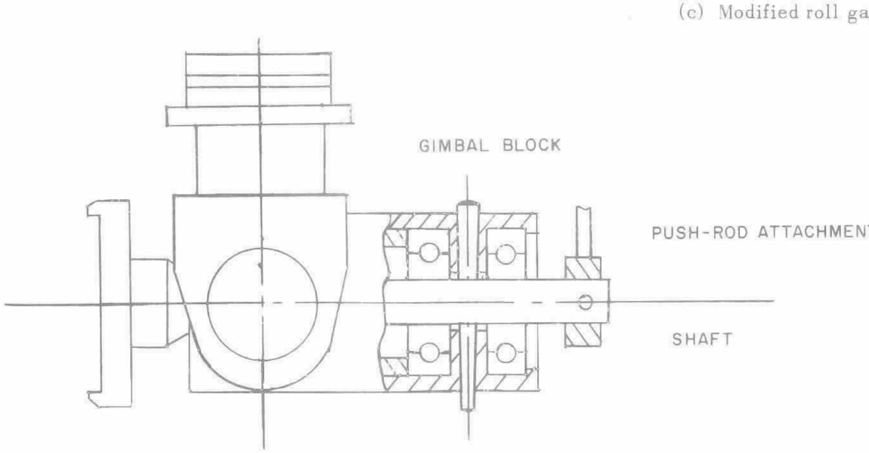

Fig. 17(a), (b), (c). Roll gage

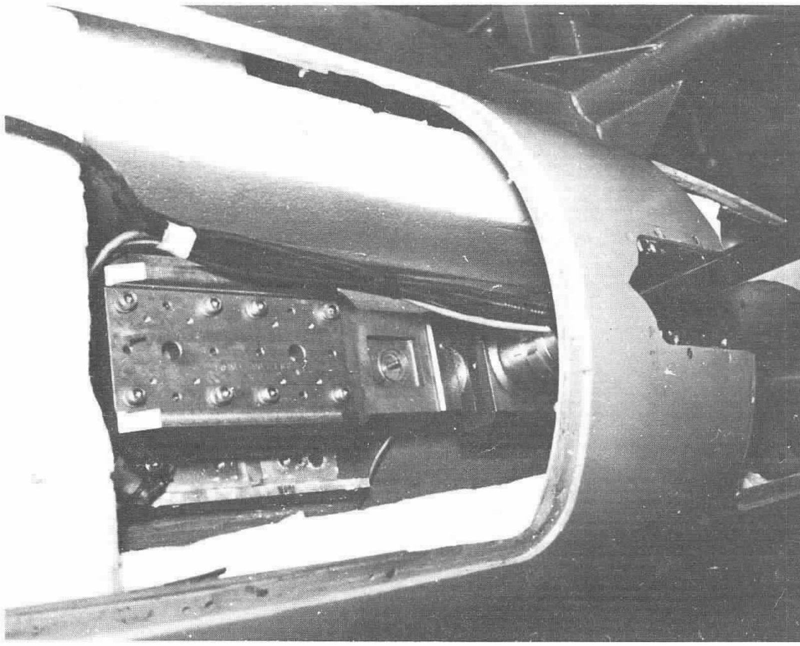

(a) Top view

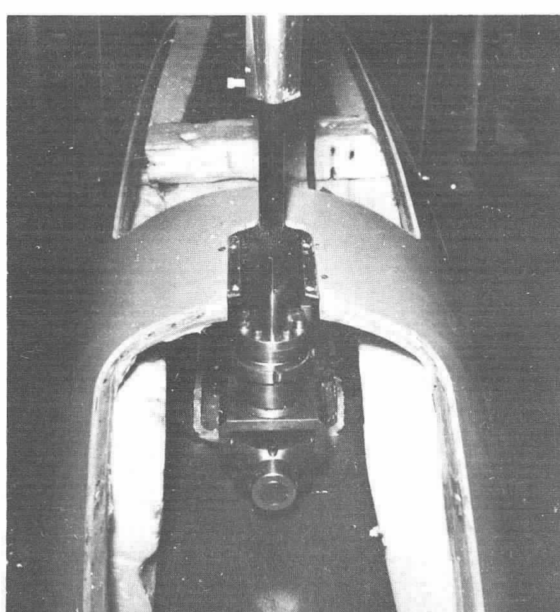

(b) Fore and aft view

Fig. 18. Gage assembly

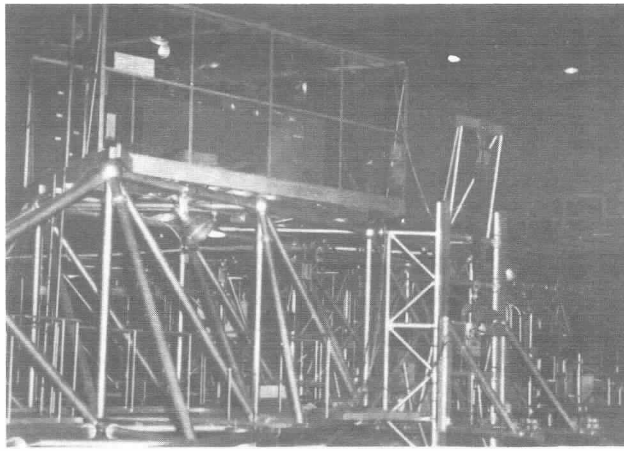

Fig. 19. Penthouse mounted on top of carriage

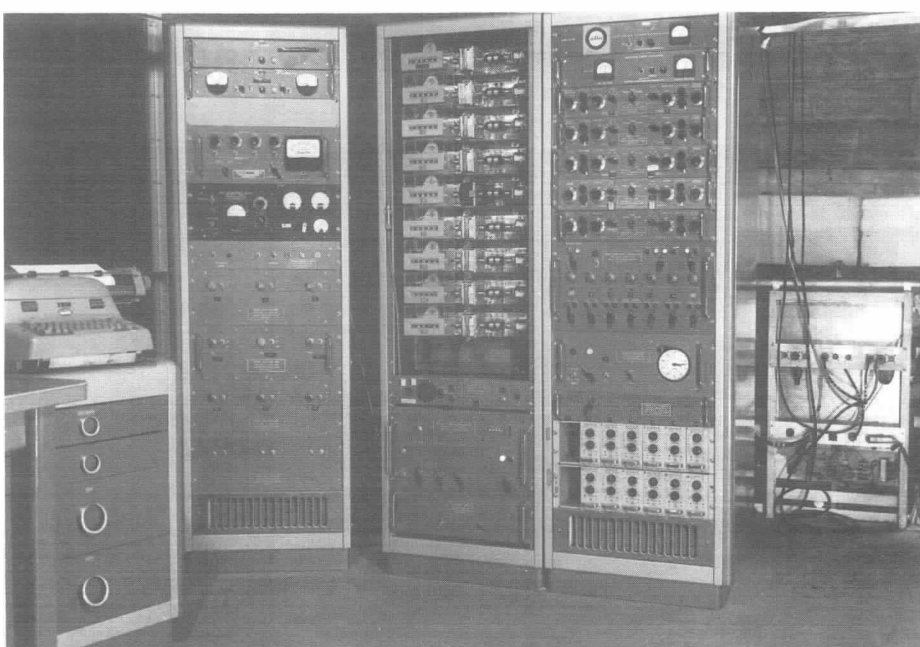

Fig. 20. Inside view of penthouse showing instrumentation

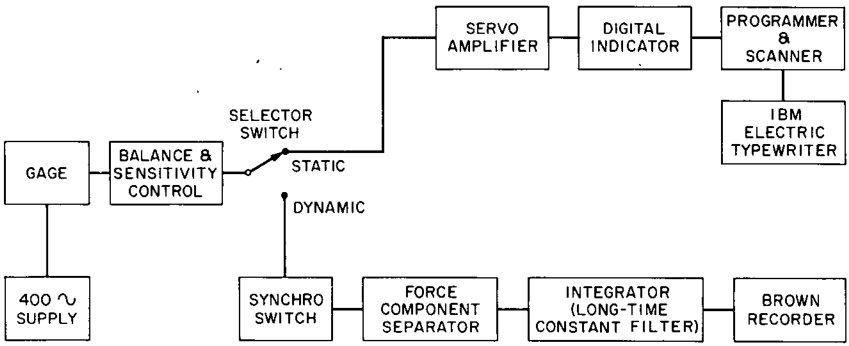

Fig. 21. Instrumentation system for Planar-Motion-Mechanism System

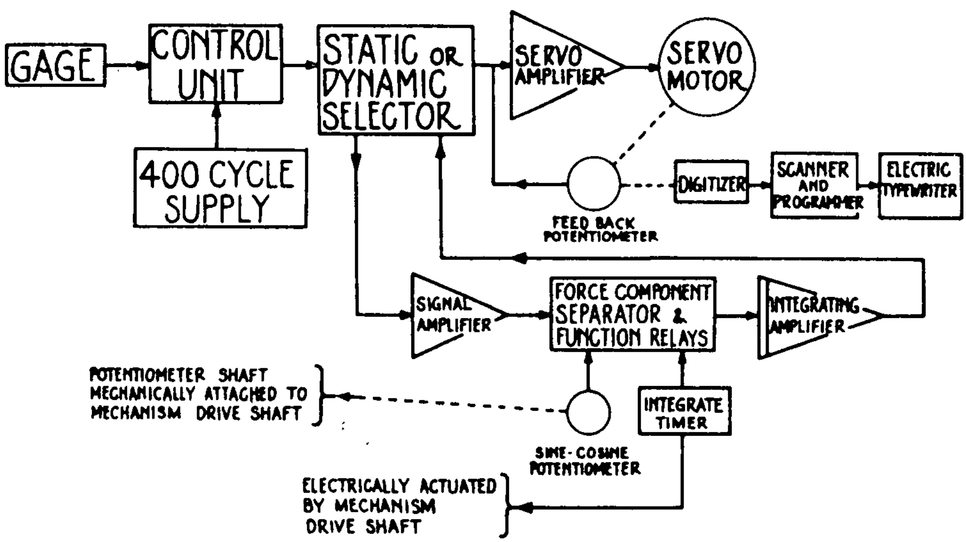

Fig. 22. New instrumentation system for static and dynamic stability tests

The roll gage assembly, shown in Figs. 17a and 17b, was modified as sketched in Fig. 17c. The longer shaft is now supported in the gimbal block by two ball bearings. For the static, heaving, and pitching tests, the shaft is attached to the gimbal block by a large taper pin. In this mode the balances and gimbal block assembly function as described in Ref. 2.

For the rolling tests, the taper pin is removed and the push-rod attachment is installed. The body can now be oscillated in roll through the roll gage located at the aft strut and the three-degree-of-freedom gimbal located at the forward strut.

The range of oscillation frequencies and frequency changing procedures for the rolling mode are the same as for the pitching and heaving modes [2].

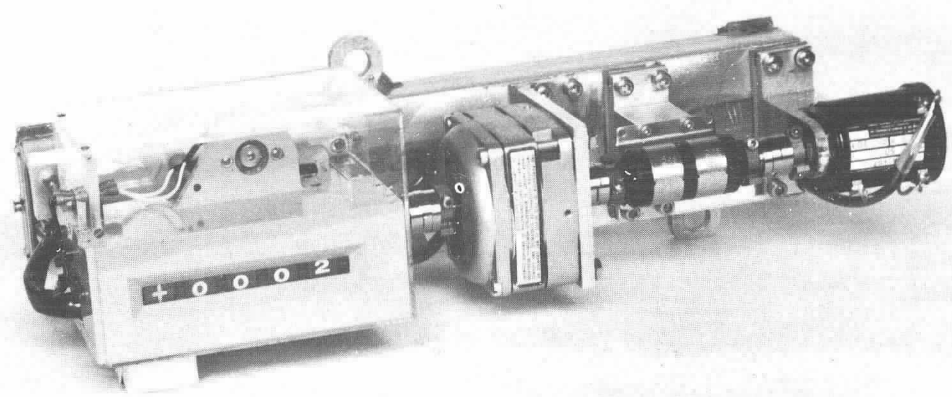

Fig. 23. Digital indicator

Instrumentation for Static and Dynamic Stability Tests – A comparison of the old and new measuring and recording systems, presented in Figs. 21 and 22, respectively, shows that both systems are essentially the same for the static stability tests. The major difference is in the method and equipment used in the dynamic tests. For completeness, however, the measuring and recording equipment used in the static and dynamic tests, shown by the block diagram in Fig. 22, will be described.

The recording equipment for the static stability tests is a digital system designed to display and read out the unique steady-state value of each force and moment sensed by the transducers for any given test condition. The system is made up of seven channels to conform to the number of gages in the model. Each channel is separate in all respects except for the power supply that it shares in common.

Briefly, each channel is essentially an automatic null-balancing system; the transducer in the gage and the digital indicator combine together in a servo system. The transducer output is balanced by a potentiometer. When a gage in the model is deflected, the resulting error signal from the transducer is amplified and drives a servo motor which positions a potentiometer to restore electrical balance, or null, to the system. The amount that the potentiometer is moved is then a measure of the force or moment applied at the gage. The various components and circuitry which constitute the recording systems are shown by the block diagram in Fig. 22.

The upper path of Fig. 22 applies to the digital system used for static stability tests. A Brown recorder could be used in place of the digital system. The term gage is used to denote the variable reluctance transducer whether it be the magnigage used with the modular force gages or the magnitorque used with the roll gages. The 400-cycle power source supplies a 4.5-volt carrier to the gage in such a manner that the current divides into two paths, one about each coil. If the core of the gage is electrically centered, the impedances of the gage halves are equal, and consequently the voltages are equal. As the core is displaced, the impedance of one gage half increases and that of the other decreases with corresponding voltage changes.

Alternating voltage from the gage passes to the balance and sensitivity control box, which contains a silicon diode bridge as well as other adjustments and refinements that are described in more detail later. The voltage is rectified by the diode bridge to produce full-wave rectified direct-current voltage. The total rectified voltage obtained across both coils is constant and is used as a reference voltage. Polarity is established by making one side of the line positive and the other negative. The voltage measured between each coil changes, however, when the gage core is displaced; the voltage across one coil increases while the other decreases an equal amount so that the reference voltage always remains constant. This is analogous to a three-wire system in which the voltage across the outside lines remains constant but the voltage from one side to the common is made variable. The feedback potentiometer, which is on the shaft of the digital indicator, is wired similarly; the voltage across the end terminals is the reference voltage and the common is attached to the potentiometer slider. When the gage core is at electrical center, the potentiometer slider is at midposition. When the gage core is displaced, an error signal results.

The error signal is fed through a mode selector switch (static or dynamic; digital or recorder) to a chopper servo-amplifier similar to that contained in the Brown recorder manufactured by Minneapolis-Honeywell Company. The chopper converts the direct-current error signal into 60-cycle alternating current. The resulting signal is amplified to drive a servo motor which in turn drives the potentiometer slider until the error signal is reduced to zero and a null-balance established.

The digital indicator, shown in Fig. 23, is the active part of the feedback loop. The assembly is made up largely of commercially obtainable components. Beginning from the left, it may be seen that there is a digitizer with a detent unit, servo motor, speed reducer, and potentiometer. The components are aligned axially and are connected together with Oldham couplings to minimize binding. The Metron speed reducer, is an antibacklash planetary gear box with a reduction of 21 to 1. It is inserted between the servo motor and 10-turn Heliopot (±0.05 linearity) so that the range of the system is ±5 turns on the potentiometer, with a little to spare. The digitizer is connected directly to the through-shaft of the servo motor. The digitizer is a unit manufactured by the Dayton Instrument Company. It is essentially a four-digit mechanical counter and plus-minus wheel, equipped with electrical contacts. Eleven wires are brought out of each decade, one for each unit and one common. These wires lead to the programmer and scanner and then to the readout equipment. The detent unit, which is integral with the digitizer, consists of a solenoid-operated star wheel. The star wheel is used to center the unit decade on a contact, when command for readout is given the solenoid is energized and the digit wheels are placed in contact with the electrical brushes.

The digital indicator operates in two modes: balancing and readout. In the balancing mode, it is part of the feedback loop, as explained earlier. In the readout mode, the servo motor is automatically stopped and the digitizer serves as a memory which stores the last reading obtained.

The scanner and programmer unit is the brain of the readout system. It serves two functions: first, introducing predetermined data such as run number, body angle, and control surface angle and secondly, scanning and sequencing the data actively obtained during the test. When a test run is made, the digital indicators are allowed to settle out at an approximately fixed reading. At command, the servo motors are automatically stopped and the scanner unit scans each channel, decomplimenting if necessary, and feeds the readings in correct sequence, one digit at a time, to the solenoid-operated IBM electric typewriter. The typewriter tabulates the data on a form specially prepared for the purpose, as shown by the reduced sample given in Fig. 24.

SUBMAP STABILITY AND CONTROL DATA SHEET
PRNC-TA. .13 (2-58)

SHEET NO. 23

MODEL 4737 | ENGINEER(S) Young-Schwarting | NOTES Strip tests top rudder and prop. off Sono 5:1 all gages except Y's

[X] HORIZONTAL [ ] VERTICAL

DATE 5-5-59 TIME 1515

RUN NO	δ	α	β	δr	δh	δs	X_1 … K	SPARE	DIR	Δt	SPEED	RPM #1	RPM #2	
2023			00	002			0001 0000 0000 0000 0000		0	05	00180	00001	00002	0 0
2024			00	-000			0015 - -0021 0016 -0070 0008 0000		0	05	10140	00002	00001	0 0
2025			02	-000			0042 -0212 0232 -0058 -0084 0044 0000		0	05	10144	00002	00001	0 0
2026			04	-000			0067 -0213 0482 -0120 -0088 0163 0000		0	05	10144	00001	00001	0 0
2027			-00	000			0022 -0207 -0012 0019 -0066 0015 0000		0	05	10157	00001	00002	0 0
2028			-02	000			0010 -0195 -0295 0110 -0056 0069 0000		0	05	10146	00001	00001	0 0
2029			-04	001			0027 -0187 -0536 0158 -0032 0190 0000		0	05	10145	00001	00001	0 0
2030			-06	001			0029 -0190 -0793 0173 -0008 0425 0000		0	05	10153	00002	00001	0 0
2031			-08	000			0032 -0188 -1041 0155 -0019 0738 00000		0	05	10153	00001	00001	0 0
2032			-12	000			0001 -0200 -1060* 0061 0062 1098* -0001		0	05	10145	00001	00001	0 0
							* after no means hit limit							
2033			00	050			0020 -0212 -0060 0111 -0063 0011 -000		0	05	10145	00001	00001	0 0
2034			02	049			0042 -0216 0186 0045 -0075 0044 -0001		0	05	10141	00001	00002	0 0
2035			04	049			0066 -0218 0427 -0004 -0085 0157 -0001		0	05	10154	00001	00002	0 0
2036			-00	049			0021 -0214 -0057 0111 -0062 -0000 -0001		0	05	10138	00001	00001	0 0
2037			-02	050			0008 -0200 -0335 0193 -0041 0056 -0002		0	05	10149	00002	00001	0 0
2038			-04	049			0021 -0198 -0580 0243 -0014 0194 -0002		0	05	10143	00001	00002	0 0
2039			00	-046			0020 -0211 0014 -0061 -0066 0008 -0001		0	05	10137	00002	00002	0 0
2040			02	-044			0040 -0211 0268 -0139 -0073 0040 -0001		0	05	10141	00002	00002	0 0
2041			04	-045			0064 -0210 0520 -0196 -0075 0157 -0001		0	05	10143	00001	00001	0 0
2042			-00	-045			0016 -0206 0018 -0062 -0057 0005 -0001		0	05	10148	00002	00002	0 0
2043			-02	-045			0010 -0194 -0254 0016 -0050 0062 -0002		0	05	10142	00001	00001	0 0
2044			-04	-045			0027 -0188 -0499 0059 -0026 0191 -0002		0	05	10148	00001	00001	0 0

Fig. 24. Typical data sheet for static and dynamic tests

As mentioned earlier, the balance and sensitivity control box contains features that are provided for the purpose of maintaining accuracy and increasing versatility of the system. Among these features are the means of checking zero, adjusting and checking sensitivity, changing zero reference, and filtering to smooth out the data.

A zero-check switch is provided to separate any change of reading due to causes other than actual gage displacement. These changes could be due to causes such as changes in value of circuit resistors or diodes. When the switch is closed, the primaries of two input transformers of the control circuit are connected in parallel so that their voltages must be equal regardless of gage core position. If the zero-check reading differs from the original value, the difference is due to changes in the control unit circuitry rather than the gage. Thus, the reading obtained on the digital indicator may be corrected by this amount. If the gage is not balanced at the time of testing due to preload or core offset, it is desirable to balance it directly. This is accomplished by a "gage zero" potentiometer which is adjusted to make the impedances across the two gage halves equal.

The "pen position" adjustment is provided to set the initial reading of the digital indicator or recorder to any desired value while the model is at rest. The usual practice for steady-state tests is to adjust the digital indicator to read zero when there are no hydrodynamic loads on the system. The setting is periodically checked before each run or group of runs to maintain the zero. The advantages of this procedure are that it provides a means for determining easily whether any changes other than hydrodynamic have occurred in the total system and it eliminates the need for subtracting arbitrary readings on each channel to obtain the net readings. The pen position adjustment is accomplished by a potentiometer which is connected in parallel with the feedback potentiometer.

A span or sensitivity adjustment is provided to establish the calibration of the digital indicator in terms of the load on the gage. The span control is a potentiometer which is placed in series with the part of the circuit that goes with the feedback potentiometer slider. Thus the unbalanced voltage resulting from displacement of the gage appears across the span potentiometer as well as any other resistors placed in series with it. The range of sensitivity varies from nearly zero to an amount somewhat in excess of that required to accommodate the maximum sensitivity of all the types of transducers used in the tests. The span potentiometer has a calibrated index and can be locked into place. However, since the control units and gages can be interchanged, the span potentiometer setting is not sufficiently accurate. Therefore a system for setting sensitivity which is independent of the transducer movement is provided. This "span check" is made by applying a step signal to simulate an actual transducer change. To do this, a precision resistor in the control box is shunted across one gage coil. The resulting span check reading on the digital corresponds to the given sensitivity and to the nominal setting on the span potentiometer.

Span control settings and span checks are usually established with the modular force gage or roll balance mounted on a calibration stand. Since all components of the measurement system are linear, the settings are determined on the basis of that required to give a reading of exactly 1000 counts on each channel for some predetermined load. As mentioned earlier, the usual sensitivity is 200 pounds for 1000 counts; however, sensitivities of twice or one-half of this amount are used from time to time, depending on the range of loads encountered in the test. The span checks for each calibration are recorded in a log book. These values have been found to hold true for any particular gage and control box combination over a period of years.

The signal coming from the gages is a fluctuating one even in steady-state tests. This is due largely to carriage vibrations which are transmitted to the model through the rigid attachment. A filter is provided in the control box to smooth this signal to obtain one steady value at the digital indicators. The filters are made up in steps so that only the amount needed for smoothing is used without needlessly sacrificing speed of response. The filter switch connects successive values of capacitance between the span potentiometer slider and one side of the feedback potentiometer. The polarity between these two points is always the same, so that electrolytic capacitors of reasonable size can be used. Since this capacitance is outside the servo feedback loop, it introduces no instability.

The recording and measuring equipment for the dynamic tests uses the same control unit, 400-cycle power supply, and digital readout or Brown recorder system. The distinguishing features are: the introduction of the signal amplifier, the force component separator, the integrating amplifier, the multiganged sine-cosine potentiometer, and the integrate timer and function relays. These components are shown by the lower leg of the block diagram of Fig. 22. They become part of the measuring and readout system when the selector switch is thrown from static to dynamic. The selector switch also selects the type of readout; that is, digital or Brown recorder. The digital system, however, is represented in Fig. 22.

The signal amplifier shown by the block diagram is a high-gain transistorized amplifier that provides accurate amplification of signals in millivoltages over the frequency range from direct current to 20 kilocycles. Some of the principle features of this amplifier are: high input impedance, and therefore negligible loading effect on transducer initiating signals, drift of less than 2 microvolts per 10 °F change in ambient temperature for the 0.1- to 30-millivolt input ranges, and for frequencies of 0 to 10 cycles per second, an equivalent input noise of about 4 microvolts peak to peak. This amplifier, the Accudata III, is manufactured by Minneapolis-Honeywell Company. Seven of these amplifiers are used in the system; one for each gage.

The multiganged sine-cosine potentiometer (eight potentiometers mounted on one shaft) is mechanically attached to the Planar Motion Mechanism driveshaft in the same manner as that used for synchronous switch, shown in Fig. 14, and rotates at the displacement frequency ω. Each sine-cosine potentiometer has a function conformity of ±0.25 percent from 0 to 360 degrees. These potentiometers are manufactured by the Beckman Heliopot Company.

The output of the signal amplifier is applied to the input of the sine-cosine potentiometer within the circuitry of the force component separator. The force component separator consists of seven channels, one for each gage. The major components of the force component separator unit are the function switch, normal-reverse switch, and function relays.

The function switch has four settings which are identified as quadrature, reset, in-phase, and calibrate. The quadrature position electrically multiplies the amplified signal from each signal amplifier with the cos ωt generated by a corresponding cosine wiper of the sine-cosine potentiometers. The in-phase position performs a similar multiplication with sin ωt. In the reset position, the feedback capacitor of the integrating amplifier is shorted out and the output voltage of the integrating amplifier is returned to its zero level. In the calibrate position, the sine-cosine wipers are disconnected and the signal is multiplied by unity instead of either sin ωt or cos ωt. The significance of this will be discussed later. The normal-reverse switch changes the polarity of the signal feeding into the sine-cosine potentiometer. This feature eliminates the requirement for knowing the static zero precisely; that is, it eliminates the need for having the transducer balanced exactly.

The product of the signal with either the sin ωt or cos ωt is fed into the integrating amplifier. This amplifier is another Accudata III operated in the open-loop mode and having a precision capacitor in the feedback loop. Again, one integrator is used for each gage in the system. The feedback capacitor has a value of 0.5 microfarad (accurate to within ±0.1 percent) and is manufactured by Arco Electronics Company. The output voltage of the integrating amplifier is fed through the contacts of the function relays; identified as "integrate" and "hold." These relays are controlled by a precision stepping switch located in the integrate timer unit. The operation of the stepping switch is controlled by a microswitch which is actuated by a sweeper mounted on the drive shaft. The number of pulses to be counted, corresponding to revolutions of the drive shaft, can be selected by a switch located on the integrate-timer unit. The home position of the stepping switch and function relays corresponds to the reset position mentioned previously. Upon being pulsed, the stepping switch operates the integrate and hold relays and then rotates an amount corresponding to the selected number of cycles. At this point the integrate relay is deenergized, opening the input to the integrating amplifier. At the same time the hold relay maintains the charge on the feedback capacitor of the integrator. The integral of the signal is therefore, the output voltage of the integrating amplifier divided by the selected time of integration. This voltage can be recorded and read out by either the digital servo system or Brown recorder.

The operation performed by this system is equivalent to determining the Fourier coefficients of the fundamental of the gage signal [10,11], as illustrated in Appendix C.

The validity of the force-component-separator and integrator system, shown in Fig. 22, has been established on the basis of controlled laboratory tests. A sinusoidal load of known amplitude and frequency (0.1 to 1.0 cycle per second) was applied to a gage. The phase angle between the gage signal and the sine-cosine potentiometer was varied known amounts over a range of ±90 degrees. The study demonstrated that the amplitude of any individual component is determined to an accuracy of better than 1 percent.

One of the main advantage of this system, over the one described in Ref. 2, is the reduction in test time for the dynamic mode (about 50 percent) and the use of the digital-readout system for recording purposes.

Typical Test Results Obtained with the System

All the hydrodynamic coefficients required in the equations of motion for submerged bodies in six degrees of freedom can be obtained with the DTMB Planar-Motion-Mechanism System. This is accomplished by appropriate orientation of the model and mode of operation of the system.

Both the linear and nonlinear coefficients associated with static stability and control are determined using the system. In the case of the rotary and acceleration derivatives, however, only the linear coefficients are determined.

The various static, rotary, and acceleration coefficients that can be evaluated using this system are presented in Appendix B and Table 2. It is believed to be pertinent, however, to include representative samples of test results obtained for each of the three classes of coefficients. Examination of these samples should provide insight not only into the nature of these coefficients but also the quality with which they can be determined by the system. Before proceeding, it is reemphasized that all of the coefficients are obtained from the explicit relationships given in Table 2.

Typical test results for coefficients of the "static" variety are shown in Figs. 25, 26, and 27. The variation of normal force and pitching moment with body angle is shown in Fig. 25 and the variation of normal force and pitching moment with stern plane angle is shown for various body angles in Figs. 26, and 27, respectively. The body-angle and plane-angle range covered in this case is only ±6 degrees. Data are, in general, obtained over a body-angle range of ±15 degrees and a control-surface angle range of ±20 to ±45 degrees, depending on the particular control surface being investigated. As indicated in the figures, the derivatives are obtained from the slopes of the appropriate curves faired through the data points. The slopes of the body-angle curves are taken through a body angle of zero and become the static stability derivatives. The slopes of the control-surface curves for zero body angle are taken through a control-surface angle of zero and become the control derivatives.

The kind of results obtained from pure heaving tests is shown in Fig. 28. The slopes of the separate in-phase force component curves are used with the formulas given to obtain the linear acceleration derivatives, the added mass $Z_{\dot{w}}$ and associated moment $M_{\dot{w}}$.

Typical results of pure pitching tests which are used to obtain (damping) force and moment derivatives are shown in Fig. 29. It may be noted that the quadrature components of force measured at each of the two struts are plotted separately. It has been found desirable to do so since the slopes of the two curves can then be substituted directly into the two formulas shown in the figure to obtain the damping force derivative Z_q and damping moment derivative M_q.

646551 O—62——28

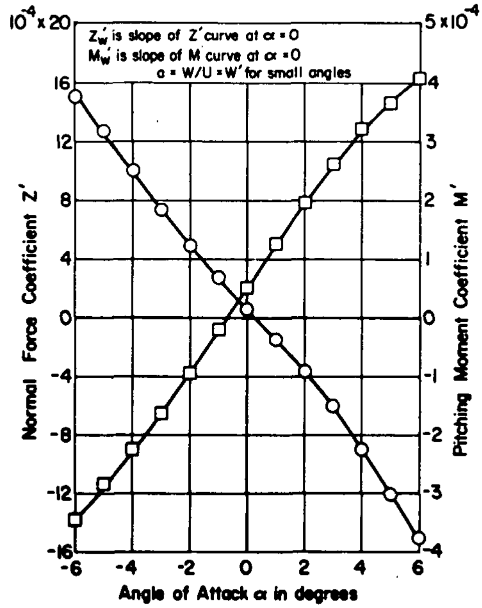

Fig. 25. Typical curves of static force and moment versus body angle

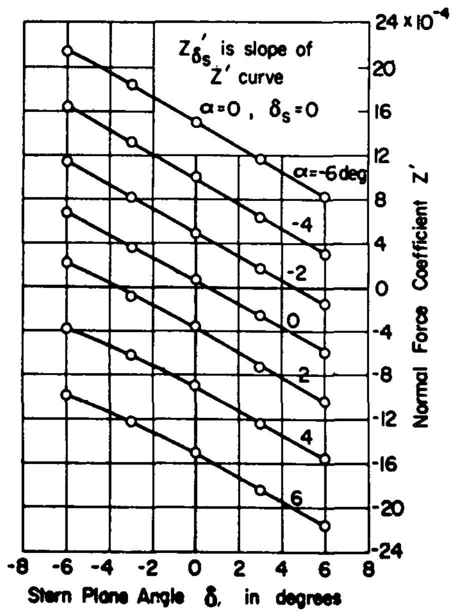

Fig. 26. Typical curves of static force versus control-surface angle for various body angles.

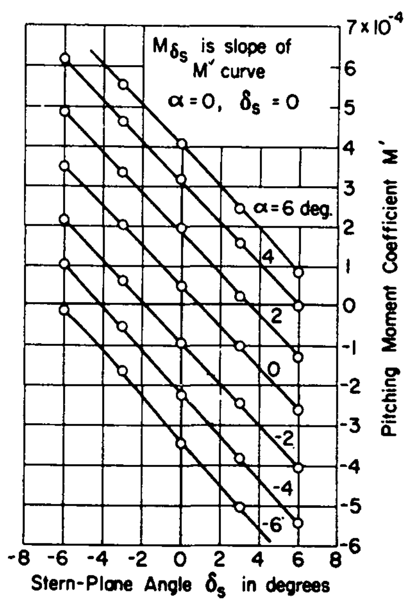

Fig. 27. Typical curves of static moment versus control-surface angle for various body angles

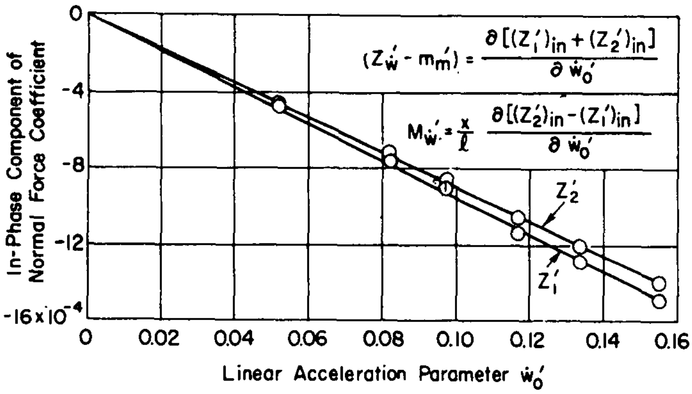

Fig. 28. Typical curves of forces versus linear acceleration amplitude from pure heaving tests used to obtain added mass (and associated moment)

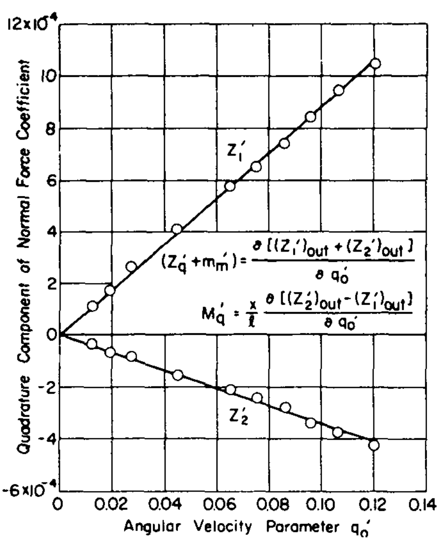

Fig. 29. Typical curves of forces versus angular velocity amplitude from pure pitching tests used to obtain damping force and damping moment derivatives

The curves of in-phase force components shown in Fig. 30 are also typical of the results obtained from pure pitching tests. Here again, the force components measured at each strut are plotted separately. The angular acceleration derivatives, the added moment of inertia $M_{\dot{q}}$ and associated force $Z_{\dot{q}}$, are obtained from the slopes of the curves using the formulas given in the figure.

Results are obtained in a similar manner for all the other hydrodynamic coefficients.

ROTATING ARM FACILITY

Another captive-model technique that has been used extensively in submerged body research, to determine explicitly the rotary coefficients for the differential equations of motion,

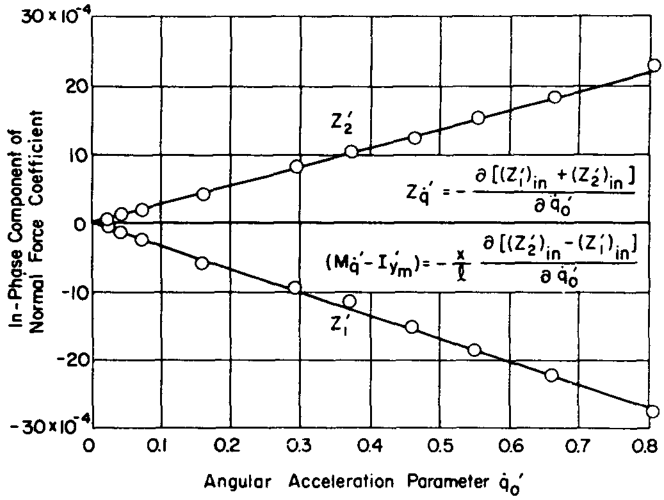

Fig. 30. Typical curves of forces versus angular acceleration amplitude from pure pitching tests used to obtain added moment of inertia (and associated force)

is the rotating arm technique [12]. In this case, the body is towed at uniform angular velocity in a circular path at different radii and the resultant forces and moments are determined for various body angles. The rotating arm technique has been used also to obtain the static-stability derivatives. In this case, the data for the various body angles are extrapolated to infinite radius and cross-plotted against the body angle. This is an indirect procedure and is generally not recommended.

The DTMB Planar-Motion-Mechanism System determines only the linear rotary derivatives. The DTMB rotating arm, using the same models, will supplement these results and provide a measure of the nonlinearities which are presently being estimated theoretically.

A detailed description of the DTMB rotating arm facility is presented in Ref. 13. For the purposes of the present paper a brief description of the main components, shown in Figs. 31 to 33, is presented herein.

The DTMB rotating arm basin is 260 feet in diameter and 21 feet deep. The arm pivots in the center on tapered roller bearings designed for centrifugal forces of 145,000 pounds. The drive system is located at the extreme end of the arm and consists of two 250-horsepower direct-current electric motors, directly coupled to two steel wheels which support the arm and run on an outer peripheral track. Each wheel is preloaded against the track by nested compression springs which provide a normal force of 61,000 pounds. A maximum steady-state speed of 30 knots can be achieved at the 120-foot radius for runs restricted to one turn. The arm, shown in Fig. 31, is a tabular aluminum structure weighing about 37,500 pounds and having natural frequencies in the vertical, horizontal, and torsional modes of greater than 3 cycles per second.

Submerged models are attached by a pair of towing struts to a model positioning apparatus, shown in Fig. 32. The positioning apparatus is attached to a carriage (Fig. 31) which can be remotely positioned along the arm to any radius from 12.5 feet to 120 feet from the

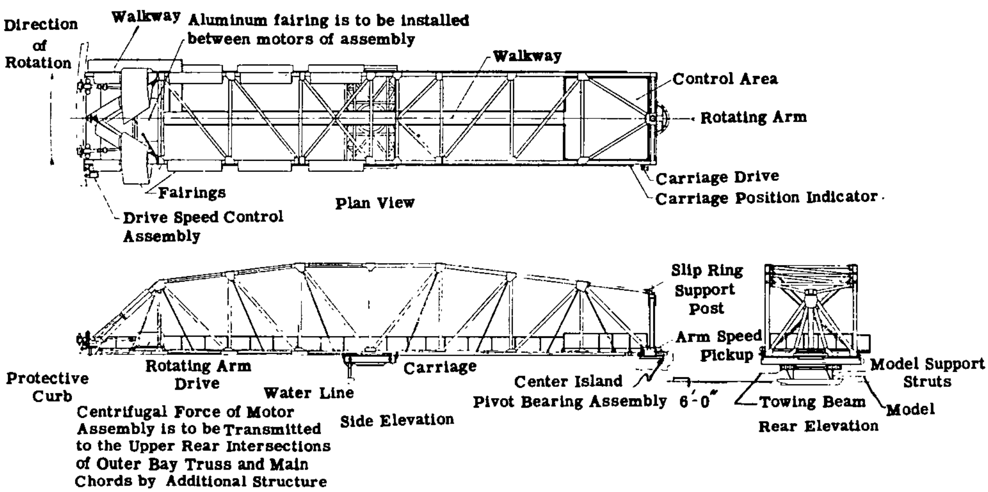

Fig. 31. Rotating arm general assembly

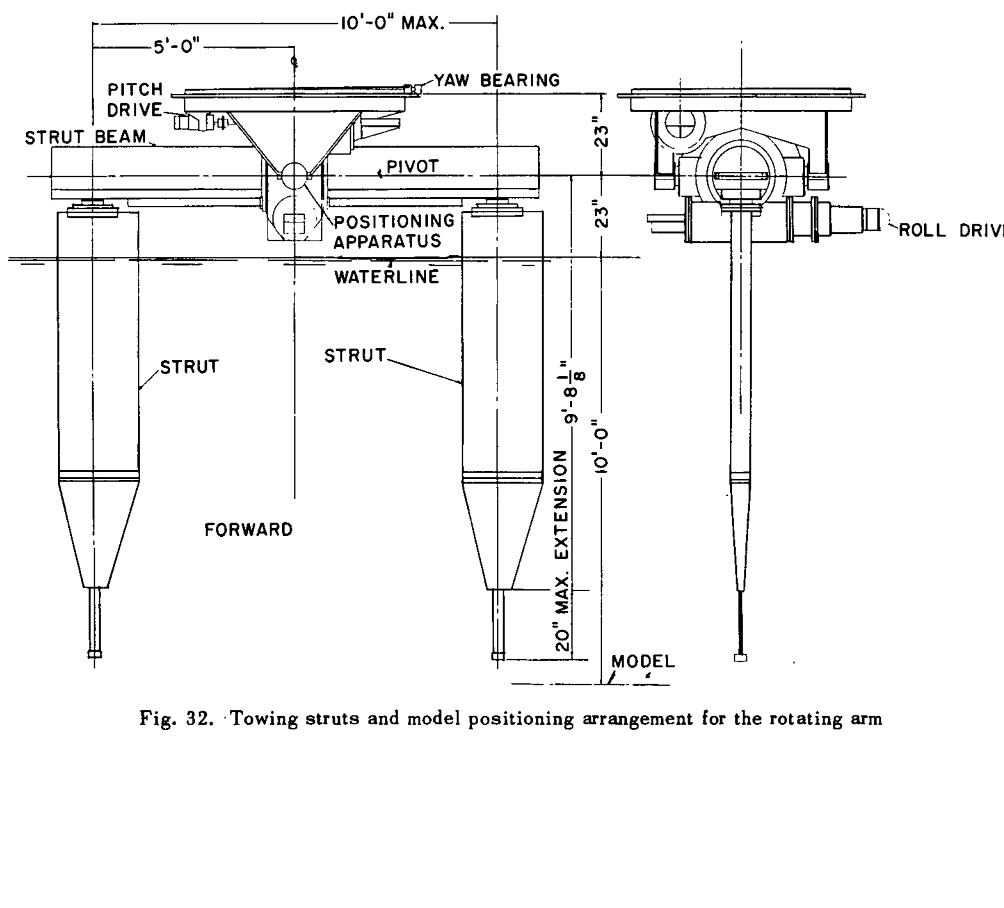

Fig. 32. Towing struts and model positioning arrangement for the rotating arm

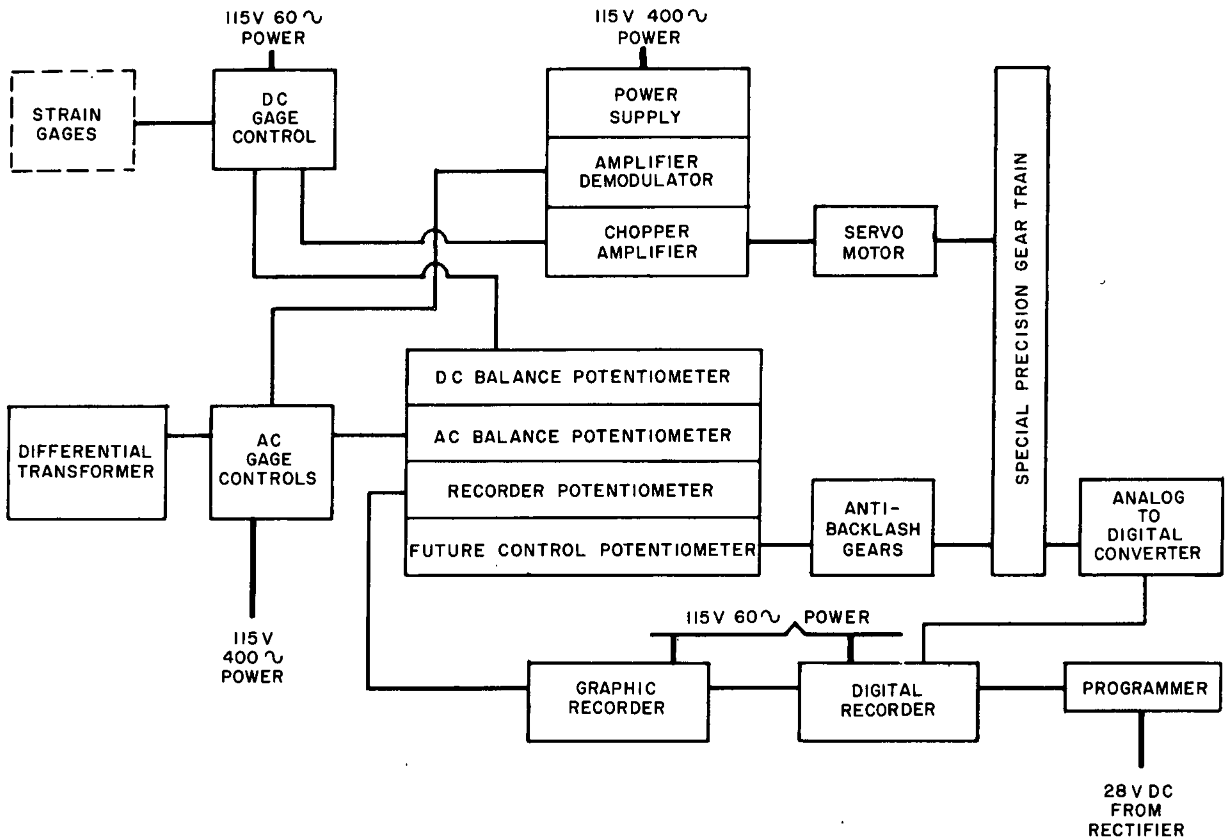

Fig. 33. Block diagram of measuring, indicating, and recording system for the rotating arm

center of the arm. The positioning apparatus is operated remotely and permits model attitudes of: yaw, plus or minus 30 degrees; pitch, plus or minus 15 degrees; and roll, 10-degree outboard, 40-degree inboard.

For yaw- and pitch-angle changes, the test location of the submerged body is unchanged. However, for roll angles, the center of roll positioning is high about the *CG* of the body, and an adjustment in radial position on the arm is necessary to maintain the proper location of the body. The positioning apparatus was made external to avoid large cutouts in the body with respect to the towing struts. Individual motor drives and position readouts are used to position the body at any attitude. Also, the support struts can be oriented with respect to the flow to minimize strut-body interference. The strut spacing is adjustable between 3.5 feet to 10 feet to accommodate various length bodies. The struts shown in Fig. 32 are similar to those used with the Planar-Motion-Mechanism System [2]. The main difference is that the upper end of the rotating arm strut has a larger chord (2.5 feet as compared to a 1.0-foot chord).

The internal balance system used with the rotating arm system is identical to that used with the Planar-Motion-Mechanism System. Likewise, the measuring, recording, and programming system, shown in Fig. 33, is essentially the same as the static-stability measuring system used with the Planar-Motion-Mechanism System.

Test runs are generally made within one turn of the rotating arm. The tangential velocity for submerged models is held constant for all radii at about 10 feet per second. For each of several discrete radii, the yaw angles (or pitch angles of a submarine model mounted on the side) is varied incrementally to investigate planar forces and moments.

MOTION ANALYSIS SIMULATOR AND FACILITY

The main purpose of any motion simulation facility is to represent, in the laboratory, the characteristics of proposed specific designs of surface ships, submarines, missiles, and other vehicles as well as the effects of the surrounding environment. Such a facility enables the designer to evaluate and improve the handling qualities or operational characteristics of a design, on the basis of established figures of merit, well in advance of construction. The facility may be used for parametric studies to investigate the importance of the various hydrodynamic coefficients and other parameters in the equations of motion. For simulating manned vehicles, the facility is used to study the responses of the human in the control loop as affected by indicators, displays, control linkage design, and environment. In addition, operating personnel can be trained well in advance of commissioning.

A simulation facility consists of a number of general-purpose electronic analog computers which are used to solve linear and nonlinear differential equations of motion such as presented in Appendix D. A general-purpose analog computer is an assembly of electronic and electromechanical units, which uses direct-current voltages as variables and can perform specific mathematical operations. When these units are connected together properly they can be used to solve mathematical equations. The independent variable is represented by time in the computer. The suitability of the computer for solving differential equations arises, therefore, from the ease with which an integration of voltage with respect to time can be achieved using a high gain direct-current amplifier having capacitance feedback [14,15]. The following basic mathematical operations, required to solve differential equations, are performed by an electronic analog computer: inversion, algebraic summation of a number of variables, multiplication by a constant, integration of a variable with respect to time, multiplication or division of one variable by another, generation of trigonometrical functions, generation of nonlinear functions, and discontinuities.

The various components that comprise the DTMB Motion Analysis and Simulator Facility are presented in Figs. 34 to 39.

A typical computer circuit diagram for a submarine in six degrees of freedom is presented in Fig. 34. The various symbols used to represent the various computer components are presented in Fig. 34d. These components are interconnected by means of a plug-in patchboard. The patchboard, therefore, represents the "mathematical" model of the system. A computer is equipment with several patchboards, and therefore one mathematical model can be stored while another study is being conducted.

The DTMB analog computer, shown in Fig. 36, consists of four general purpose computers, manufactured by the Midcentury Instrumatic Corporation, and one analog computer manufactured by the Reeves Instrument Company. This facility presently consists of 168 operational amplifiers. (The number of operational amplifiers is usually used to express the size of a facility.) In addition, auxiliary equipment such as diode function generators, white-noise generators, X-Y plotting boards, two 8-channel Sanborn recorders, strip-chart recorders, and various instrument displays are available. The present facility will be expanded shortly to about 300 operational amplifiers when several new computers are procured. With this addition, the facility will be capable of handling, simultaneously, two six-degree-of-freedom submarine studies as well as other small problems.

Studies which involve the human operator as part of the closed loop are performed using the submarine simulator facility shown in Figs. 37 and 38. The simulator consists of cube-shaped cab (about 7 feet x 7 feet x 7 feet) capable of turning on a single axis equivalent to the pitch axis of a submarine. It is hoped that an additional degree of freedom, to simulate the rolling motion of the submarine, will be added in the near future. The cab contains two control stations, each equipped with an aircraft-type control stick (stick-wheel) and the necessary display instruments. The motion of the cab is governed by an electrohydraulic servo system receiving inputs from the analog computer. A block diagram of this circuit is presented in Figs. 34c and 39.

A comparison of the submarine control cycle with the simulator control cycle, presented in Fig. 35, shows that the cab constitutes one link in a complete submarine simulator control loop which involves the human operator. The equations of motion set up on the analog computer (mathematical model) constitute another link in the control loop. Movement of the control stick in the cab produces inputs to the computer which then calculates the resultant path of the submarine. The submarine attitude angle, depth, depth error, and plane angles are displayed by the instruments and the cab rotates to the computed pitch angle. Simultaneously, a graphical record of the submarine trajectory and other pertinent information is recorded by a multichannel recorder.

The Motion Analysis and Simulator Facility in combination with the concept of the definitive maneuver provides a powerful tool for studying the handling qualities of submarines. Several of the typical definitive maneuvers, shown in Figs. 40 to 43, are performed using this facility to provide numerical measures of the inherent characteristics of submarines.

The meander maneuver, shown in Fig. 40 provides numerical measures of the dynamic stability in the vertical plane; such as, time to damp to one-half amplitude $t_{1/2}$, damping ratio c/c_c, and damped period. The overshoot maneuver also shown in Fig. 40 provides

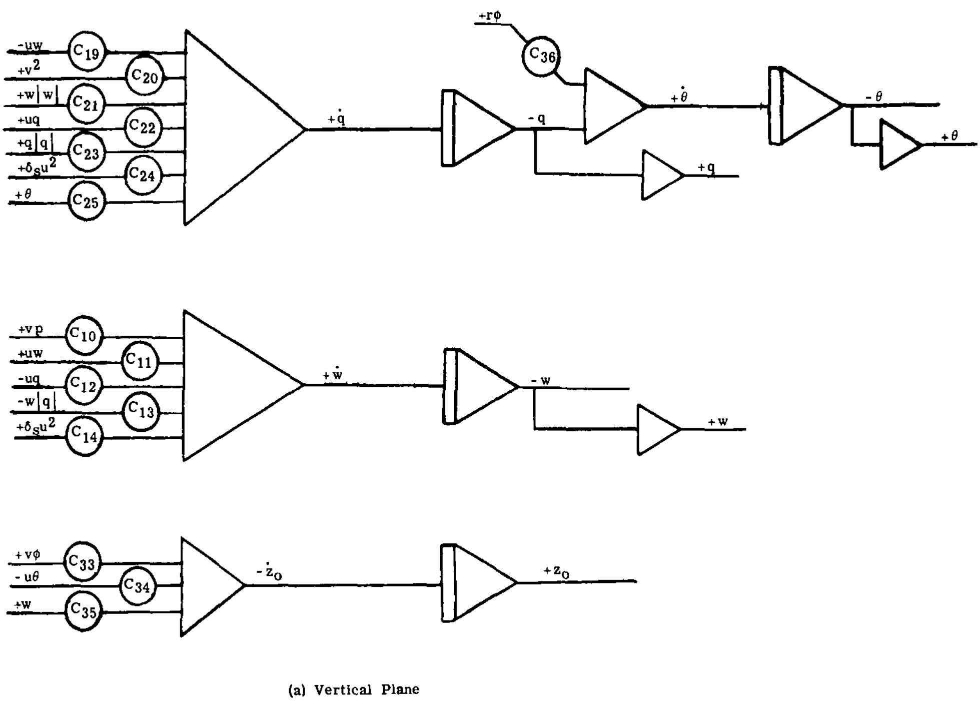

(a) Vertical plane

Fig. 34 – Analog computer diagram of submarine equations

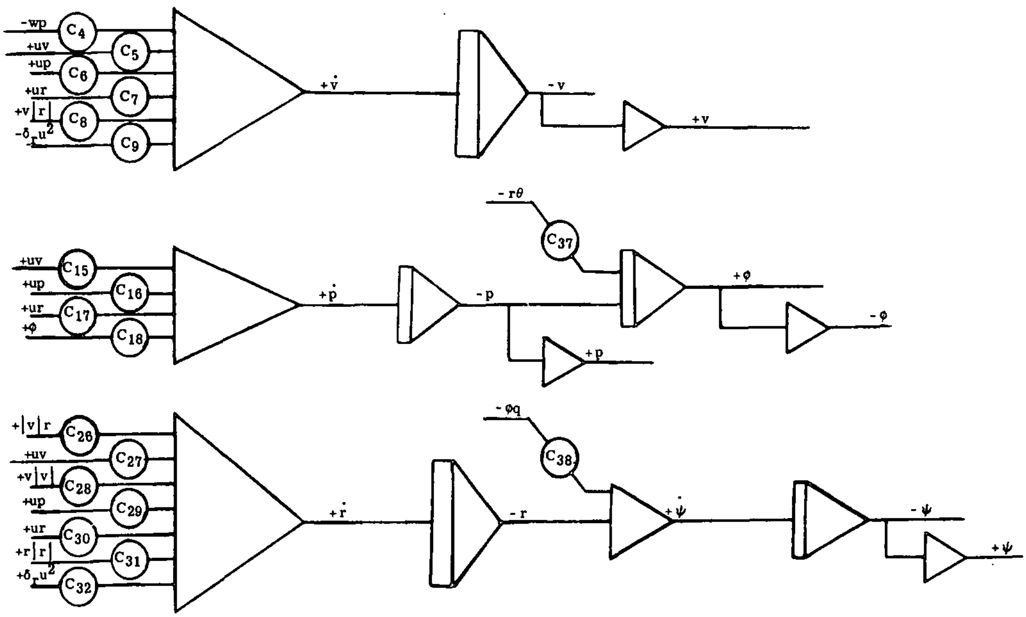

(b) Horizontal Plane

(b) Horizontal plane

Fig. 34 — Analog computer diagram of submarine equations (continued)

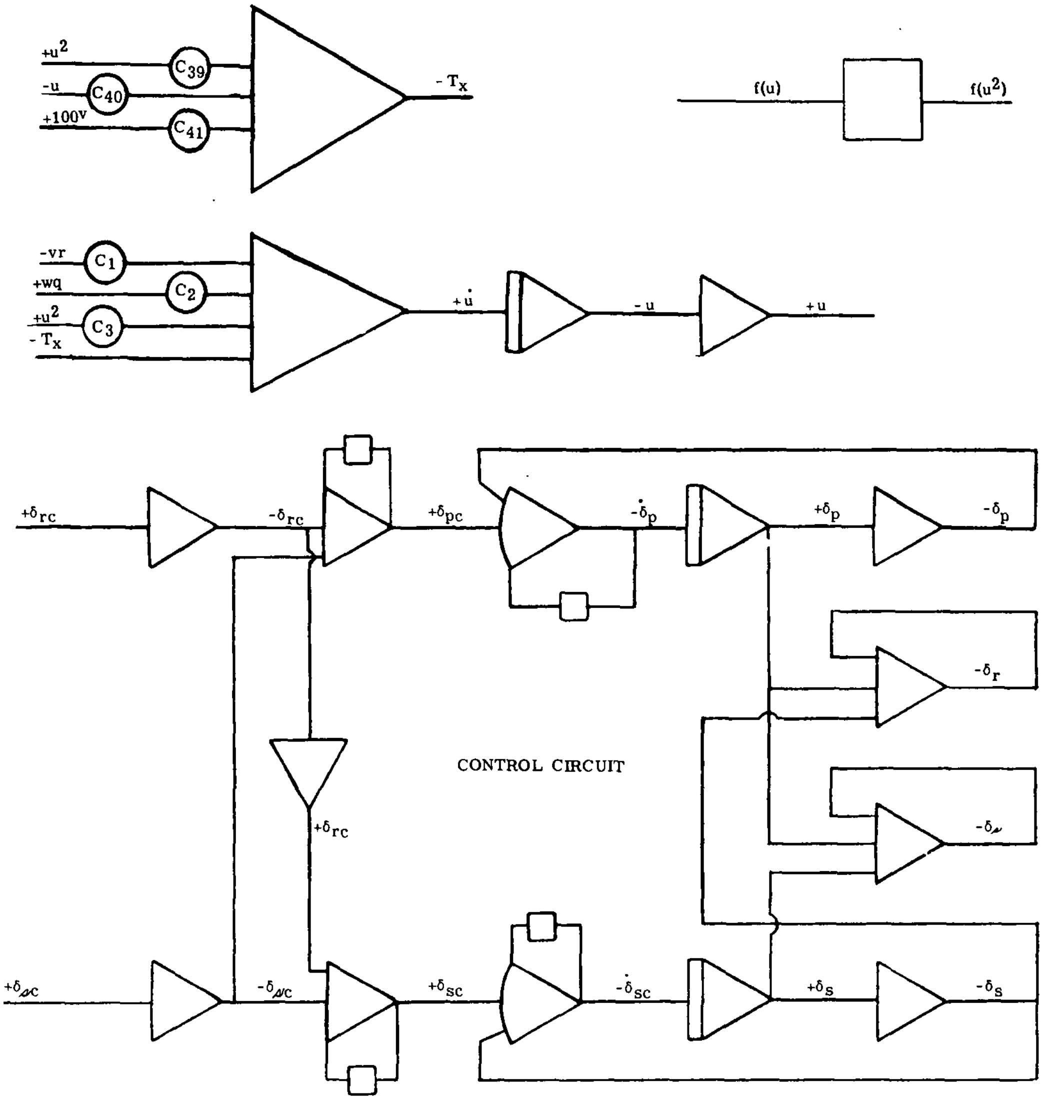

$$\delta_{pc} = \delta_{\mathscr{s}c} + \delta_{rc}$$

$$\delta_{sc} = \delta_{\mathscr{s}c} - \delta_{rc}$$

$$\delta_{\mathscr{s}} = \frac{1}{2}(\delta_p + \delta_s)$$

$$\delta_r = \frac{1}{2}(\delta_p - \delta_s)$$

where

$\delta_{\mathscr{s}c}$, δ_{rc}	are effective diving planes and rudder ordered angles
δ_{pc}, δ_{sc}	are ordered angles to port and starboard shafts
δ_p , δ_s	are actual angles of port and starboard shafts
$\delta_{\mathscr{s}}$, δ_r	are effective diving plane and rudder angles which would produce forces and moments equivalent to deflection angles of stocks

(c) Thrust representation, axial force and control circuit diagram

Fig. 34 – Analog computer diagram of submarine equations (continued)

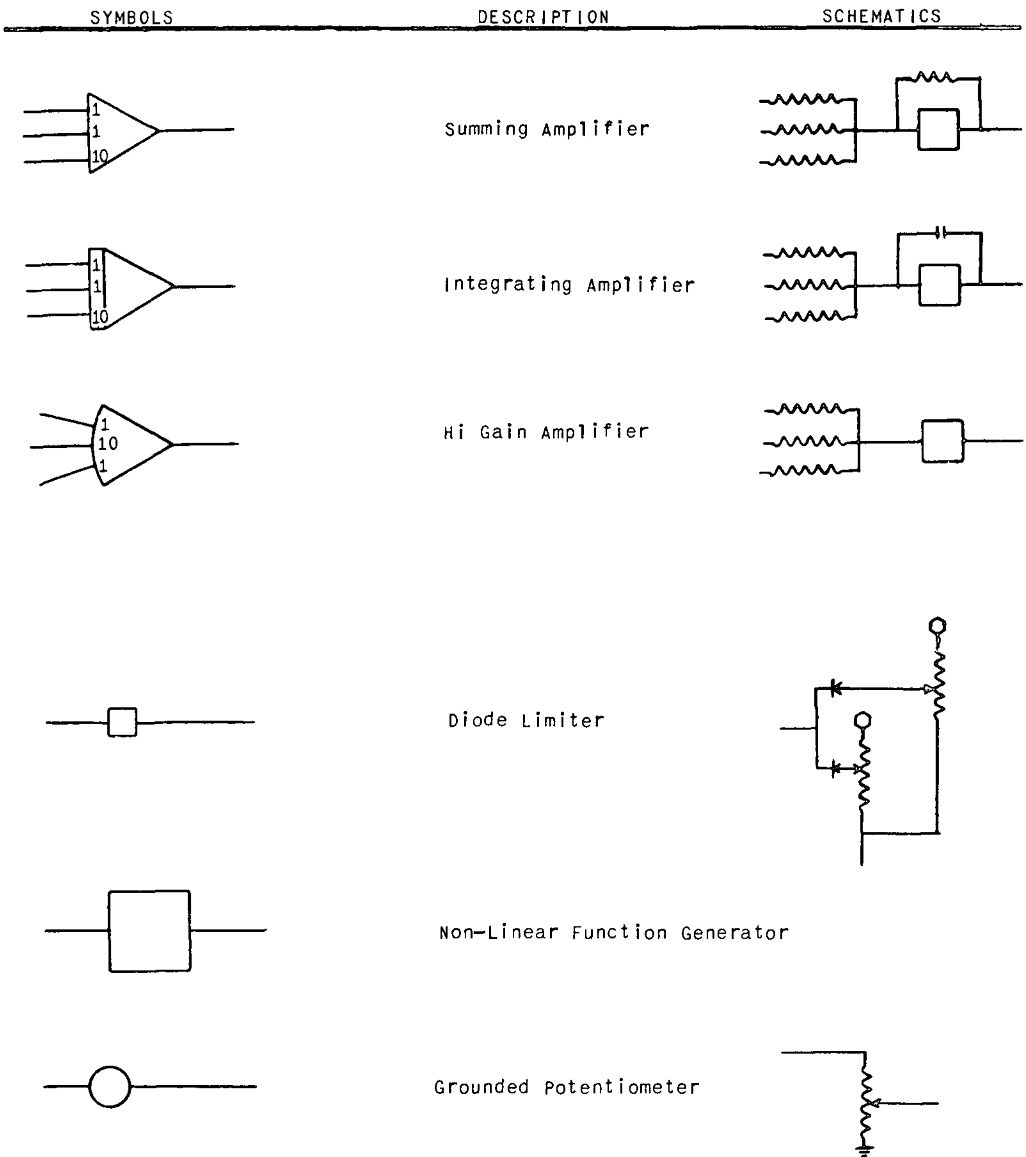

(d) Description of symbols used in analog computer diagrams

Fig. 34 – Analog computer diagram of submarine equations (continued)

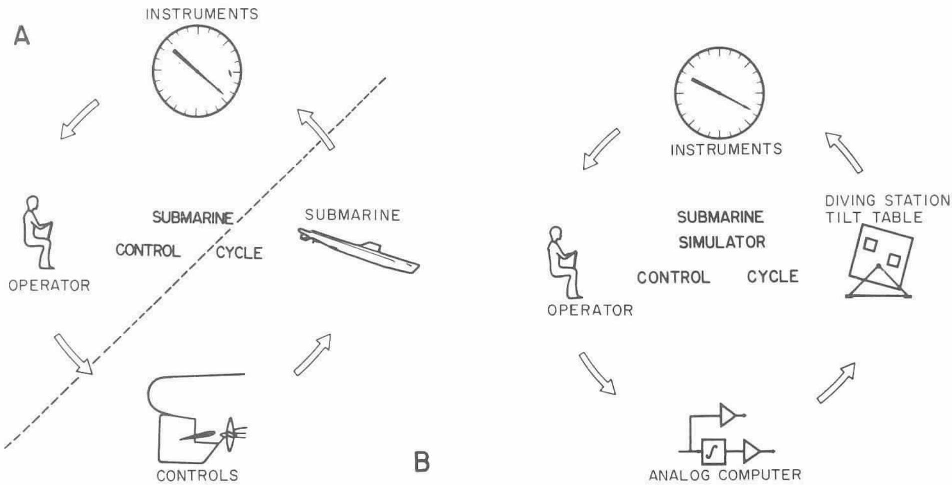

(a) Submarine control cycle (b) Simulator control cycle

Fig. 35. Comparison between submarine control cycle and simulator control cycle

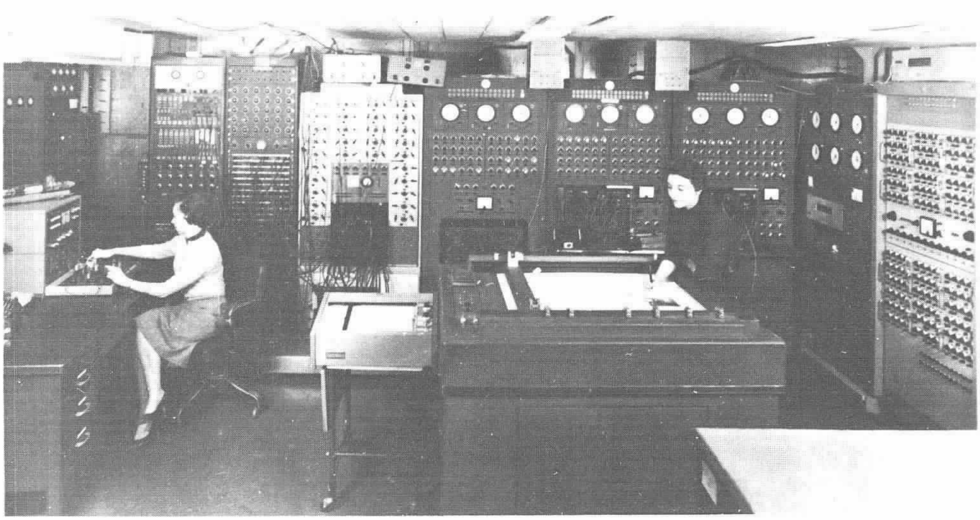

Fig. 36. DTMB analog computer facility

numerical measures of control effectiveness, such as time to reach execute, overshoot angle in the vertical plane, and overshoot depth in the vertical plane. A similar maneuver, such as shown in Fig. 42, can be used to define the ability to initiate and check a course change in the horizontal plane. The results of the Dieudonne spiral maneuver shown in Fig. 41 provides some measure of the inherent dynamic stability in the horizontal plane. These results are also indicative of the course-keeping characteristics of the submarine. Steady-turn studies such as shown in Fig. 43 provide numerical measures such as tactical diameter, advance, transfer, time to change heading 90 to 180 degrees, and loss of speed in the turn.

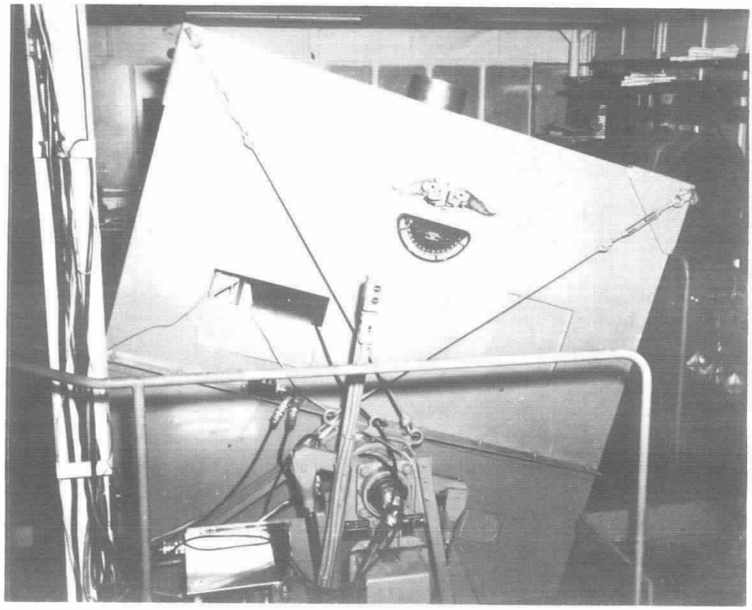

Fig. 37. DTMB submarine simulator facility

Definitive maneuvers which provide measures of the capabilities of the submarine tempered by the existence of a human operator or automatic control in the control loop can also be performed using the facility. Maneuvers such as depth-keeping and course-keeping, under various environmental conditions, provide numerical measures such as rms depth or course error, percent time on target, degrees traveled by control surfaces, and maximum values of these variables. Various other maneuvers such as limit-dives and emergency-recovery maneuvers also can be performed in the laboratory and evaluated before the submarine is built.

Instrumentation studies, which are in the nature of human engineering, can be carried out using the submarine simulator. The effect of various displays, indicators, lighting, and other devices on the performance of the submarine can be evaluated.

Thus, it can be seen that the DTMB Motion Analysis and Simulator Facility is a powerful and versatile design and research tool for the study and analysis of stability and control problems.

FREE-RUNNING MODEL TECHNIQUE

The free-running model technique has been used extensively in the past in studying the turning and maneuvering characteristics of surface ships [4]. With the emphasis that has been placed the performance of high-submerged-speed submarines, the necessity for turning data from submerged model tests has become more important. Early submerged maneuvering tests, in the vertical and horizontal planes, conducted at the David Taylor Model Basin employed a specially constructed 5-foot model provided by NACA. The model was powered electrically and controls were operated by compressed air through a flexible tubing which trailed astern of the model. Model trajectories were obtained, by photographing the movements of the model

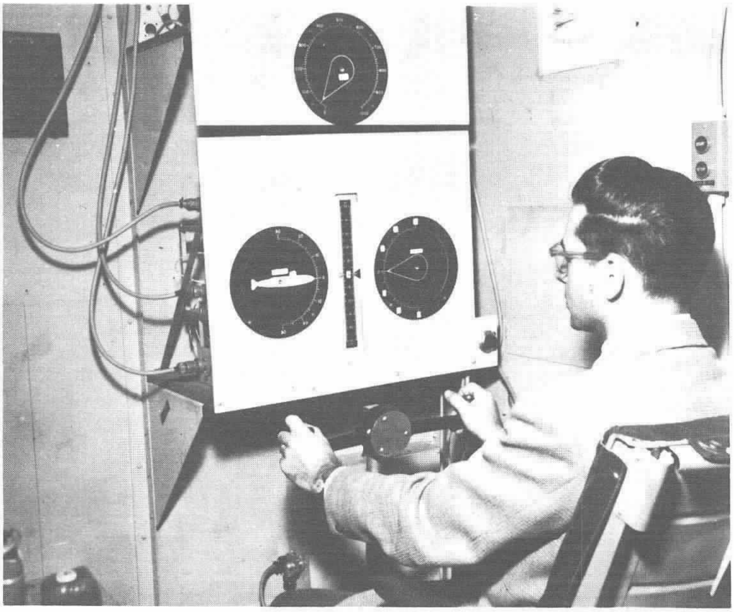

(a) Starboard control stick and display

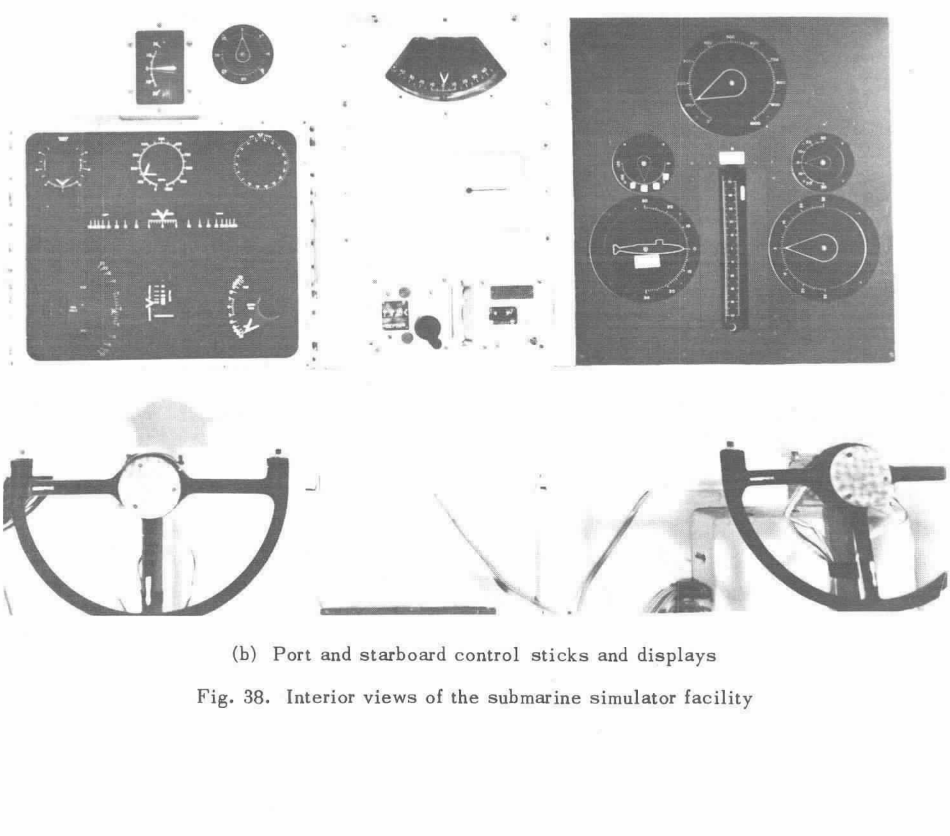

(b) Port and starboard control sticks and displays

Fig. 38. Interior views of the submarine simulator facility

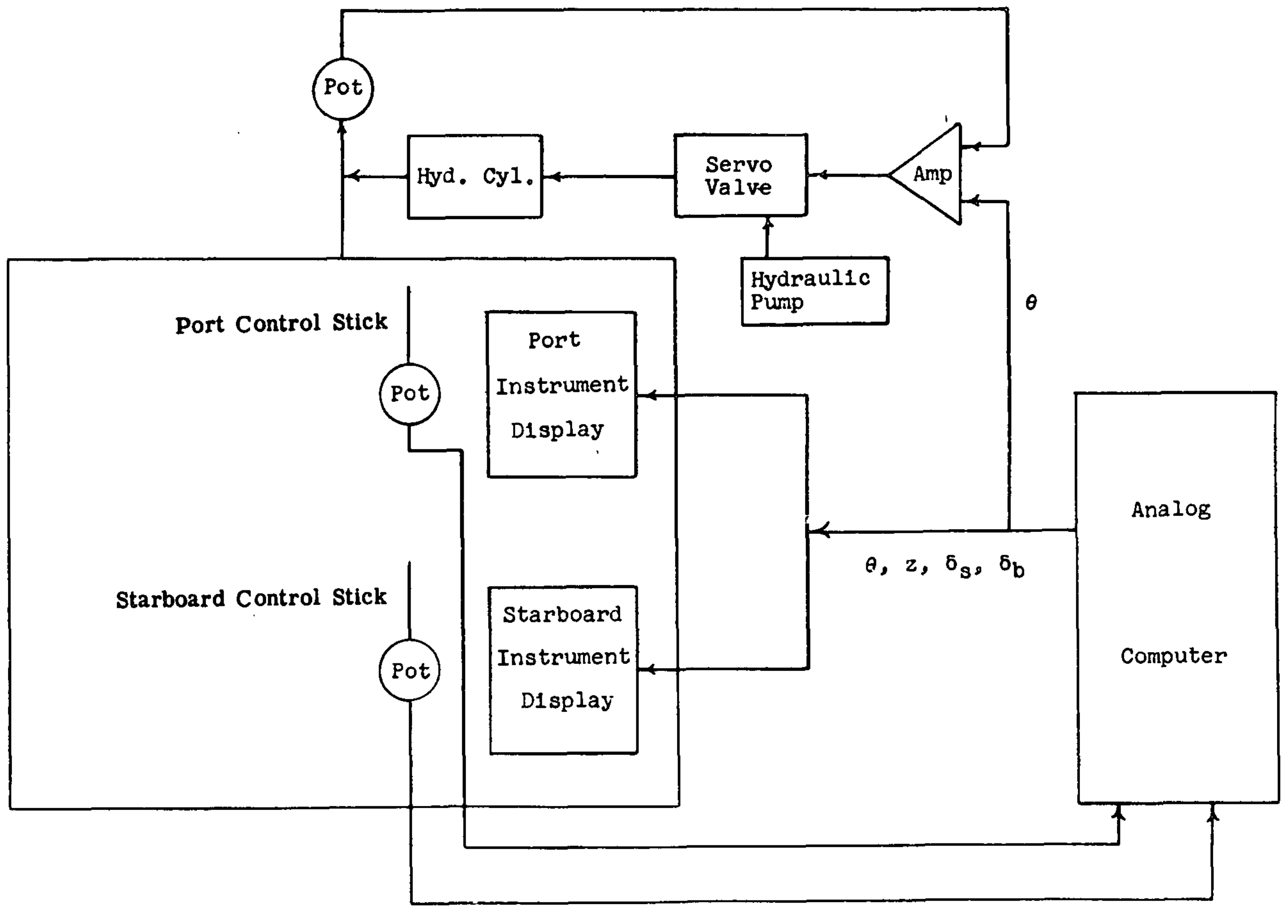

Fig. 39. Block diagram of the simulator circuit

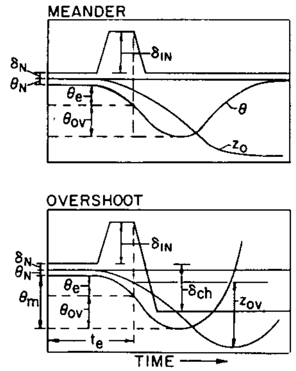

Fig. 40. Typical meander and vertical overshoot maneuvers (definitive maneuvers)

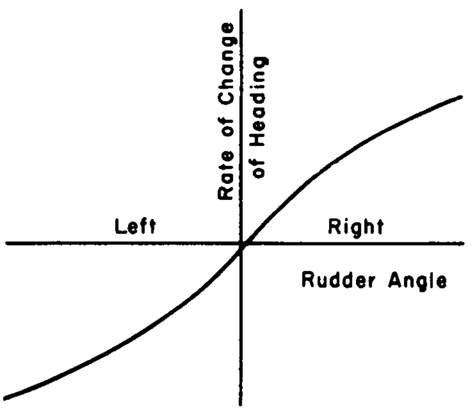

(a) Stable ship

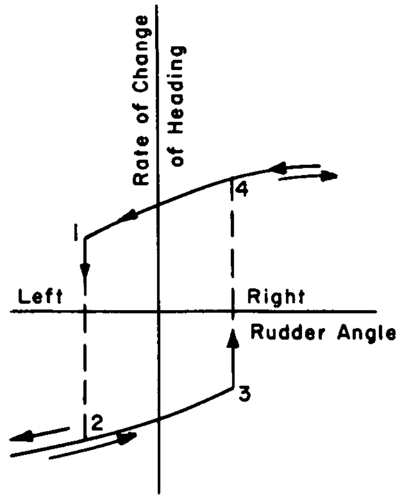

(b) Unstable ship

Fig. 41. Typical curves from spiral maneuvers

relative to a grid attached to the towing carriage, using cameras mounted inside the model. The main objections to this system are that it required an expensive model and that the excessive drag resistance of the tubing affected the maneuvering characteristics of the model.

With recent advances in electronic and electromechanical instrumentation, and waterproofing techniques, it became possible to perfect the free-running model technique using the standard 20-foot (nominal) submerged models used for both resistance and propulsion tests and stability and control tests.

The free-running submarine model tests are presently being performed in the J-basin at DTMB. Techniques have been developed so that these tests can be conducted in the new Maneuvering Basin using a model that is internally programmed and has internal recording equipment.

646551 O—62——29

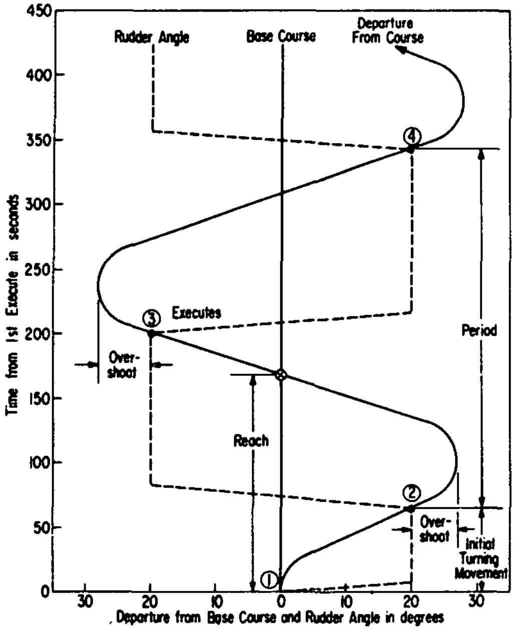

Fig. 42. Horizontal overshoot maneuver

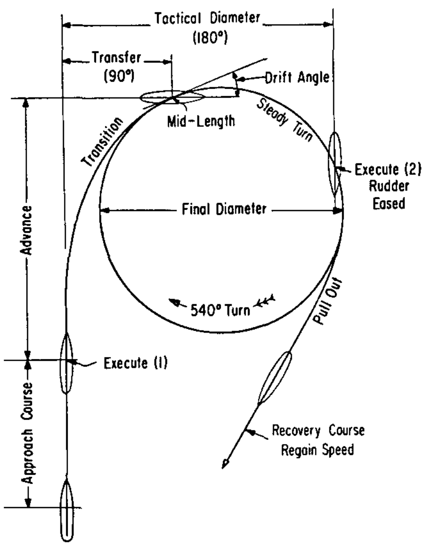

Fig. 43. Turning circle maneuvers

For the submerged tests in the J-basin, the model is provided with watertight equipment (propulsion motors, actuators, and gyros) and is ballasted so as to have only a slight reserve buoyancy. The final displacement and trim is achieved by means of the bow and stern ballast tanks. The power and control cables emerge from the model through a hollow faired tube and are supported by an overhead follower boom controlled from the carriage. The cable runs over a pulley and has a counterweight so arranged that the cable feeds out as the model submerges. A lightweight framework secured to the top of the faired tube supports flashing neon lights used in photographing (using overhead cameras) the turning path of the model. Portable control boxes are provided for both the rudder and stern plane so that the most desirable locations on the carriage could be used. The control boxes actuate waterproofed-rotary actuators, manufactured by Universal Match Corporation, which are mechanically linked to the rudders and stern planes. A trim angle indicator also is provided to simplify the work of the stern plane operator as it provides a faster and more sensitive indication then could be estimated visually. This information is obtained from a Minneapolis-Honeywell vertical gyro Type GG 33B-2 which is located in the model. The heading and rate of change of heading data are provided by a Humphrey Model FG01-0203 gyro and a Humphrey Model RG03-0117-1 gyro, respectively, and are of value to the operator of the rudder control in obtaining a straight approach course.

At the beginning of each run the model is floating with only the top of the bridge fairwater projecting out of the water. After the model has attained the desired test speed, it is maneuvered down to the test depth by means of the stern diving planes. The definitive maneuvers shown in Figs. 41 to 43, are then performed to evaluate the handling qualities of the submarine in the horizontal plane.

ACKNOWLEDGMENT

The DTMB Planar-Motion-Mechanism System was conceived and developed jointly by the author and Mr. Morton Gertler, both members of the staff of the Hydromechanics Laboratory of the David Taylor Model Basin. Patent proceedings have been initiated in behalf of the United States (Navy Department Navy Case Number 28, 121; Serial No. 817, 002) with the names of Messrs. Goodman and Gertler as originators of the system. The originators wish to express their gratitude to those members of the Industrial Department of the Model Basin whose contributions and efforts in the design and construction of components made the ultimate system possible. Particular thanks are due to Messrs. M. W. Wilson, and R. G. Hellyer of the Industrial Department for their aid in developing the instrumentation system and the roll oscillation system, respectively. The author is also grateful to Mr. Morton Gertler for his contributions to the development and application of the concepts of the definitive maneuver for evaluating handling qualities.

REFERENCES

[1] Gertler, M., and Gover, S.C., "Handling Quality Criteria for Surface Ships," paper presented at the Meeting of the Chesapeake Chapter of the Society of Naval Architects and Marine Engineers on May 2, 1959

[2] Gertler, M., "The DTMB Planar-Motion-Mechanism System," paper presented at the Symposium on the Towing Tank Facilities, Instrumentation and Measuring Technique on September 22-25, 1959

[3] Orlik-Ruckemann, "Methods of Measurement of Aircraft Dynamic Stability Derivatives," National Research Council of Canada Aeronautical Report LR-254

[4] Gover, S.C., "Free-Running Model Techniques for the Evaluation of Ship-Handling Qualities," David Taylor Model Basin Report 1350, July 1959

[5] Bird, J.D., Jaquet, B.M., and Cowan, J.W., "Effect of Fuseage and Tail Surfaces and Low-Speed Yawing Characteristics of a Swept-Wing Model as Determined in the Curves-Flow Test Section of the Langley Stability Tunnel," NACA TN 2483, Oct. 1951

[6] MacLachlan, R. and Letko, W., "Correlation of Two Experimental Methods of Determining the Rolling Characteristics of Unswept Wings," NACA TN 1309, May 1947

[7] Lamb, Sir Horace, "Hydrodynamics," Sixth Edition, Dover Publications

[8] Lopes, L.A., "Motion Equations for Torpedoes," NavOrd Report 2090, NOTS 827, U.S. Naval Ordnance Station, Inyokern, Feb. 1954

[9] Strumpf, A., "Equations of Motion of a Submerged Body with Varying Mass," Davidson Laboratory Report 771, May 1960

[10] Beam, B.A., "A Wind Tunnel Test Technique for Measuring the Dynamic Rotary Stability Derivatives Including the Cross Derivatives at Subsonic and Supersonic Speeds," NACA Report 1258, 1956

[11] Tuckerman, R.G., "A Phase-Component Measurement System," David Taylor Model Basin Report 1139, Apr. 1958

[12] Fried, W., "A Rotating Arm for Towing Models of Ships and Other Forms in Circular Paths," Experimental Towing Tank Report 299, Feb. 1946

[13] Brownell, W.F., "A Rotating Arm and Maneuvering Basin," David Taylor Model Basin Report 1053, July 1956

[14] Johnson, C.L., "Analog Computer Techniques," New York:McGraw-Hill, 1956

[15] Wass, C.A.A., "Introduction to Electronic Analogue Computers," New York:McGraw-Hill, 1956

APPENDIX A

Derivation of Phase Angle Required Between Struts for Pure Pitching Motion

The condition that must be satisfied to obtain a pure pitching motion for a body moving through a fluid is that the pitch angle varies with time while the angle of attack α, measured at the CG, is maintained equal to zero at all times. The motion is one in which the body CG moves in a sinusoidal path, with the longitudinal body axis tangent to the path, as shown in Fig. 3c. This motion in some respects is similar to that produced by a rotating arm.

The system that will be analyzed uses a slider crank mechanism having a large ratio of length of connecting rod to eccentricity. There is no appreciable error introduced, therefore, by assuming that the motion is sinusoidal for purposes of analysis. Referring to the notation and schematic diagram shown in Fig. 5, the motion of the forward and aft struts (taken with respect to the midposition of the forward strut) can be expressed as follows:

$$z_1 = a_1 \sin \omega t \tag{A1}$$

$$z_2 = a_2 \sin (\omega t - \phi_s) \tag{A2}$$

where the crank arms a_1 and a_2 are assumed to be variables. The vertical displacement of the body CG is, therefore,

$$z_o = \frac{x_2 z_1 + x_1 z_2}{b} . \tag{A3}$$

Expanding Eq. (A3) results in

$$z_o = \frac{a_1 x_1}{b} \left[\left(\frac{x_2}{x_1} + \frac{a_2}{a_1} \cos \phi_s \right) \sin \omega t - \frac{a_2}{a_1} \sin \phi_s \cos \omega t \right] \tag{A4}$$

where the strut spacing with respect to the body CG, x_1, and x_2 are assumed also to be variables. The vertical velocity of the body CG can be obtained by differentiating Eq. (4) and expressed as

$$\dot{z}_o = \frac{a_1 x_1 \omega}{b} \left[\left(\frac{x_2}{x_1} + \frac{a_2}{a_1} \cos \phi_s \right) \cos \omega t + \frac{a_2}{a_1} \sin \phi_s \sin \omega t \right] . \tag{A5}$$

For the case of pure pitching the struts are out of phase with each other, and a body pitch angle results and can be expressed in terms of the motion of each strut as

$$\theta = \frac{z_2 - z_1}{b} \tag{A6}$$

or expanding:

$$\theta = - \frac{a_1}{b} \left[\left(1 - \frac{a_2}{a_1} \cos \phi_s \right) \sin \omega t + \frac{a_2}{a_1} \sin \phi_s \cos \omega t \right] . \tag{A7}$$

The vertical velocity of the CG with respect to the inertial axes can be written as

$$\dot{z}_o = w \cos \theta - u \sin \theta \tag{A8}$$

and for small angles, where $\cos \theta = 1$, $\sin \theta = \theta$, and $u = U$, can be simplified to

$$\dot{z}_o = w - U\theta. \tag{A9}$$

Also, since $w/U = \alpha$ (for small angles), Eq. (A9) can be restated as

$$\dot{z}_o = U(\alpha - \theta). \tag{A10}$$

As stated previously, the primary condition that must be satisfied for pure pitching motion is that $\alpha = 0$. Equation (A10), therefore, reduces to

$$\dot{z}_o = -U\theta. \tag{A11}$$

Substituting Eqs. (A5) and (A7) into Eq. (A11) results in

$$\frac{\omega x_1}{U}\left[\left(\frac{x_2}{x_1} + \frac{a_2}{a_1}\cos\phi_s\right)\cos\omega t + \frac{a_2}{a_1}\sin\phi_s\sin\omega t\right]$$

$$= \left[\left(1 - \frac{a_2}{a_1}\cos\phi_s\right)\sin\omega t + \frac{a_2}{a_1}\sin\phi_s\cos\omega t\right]. \tag{A12}$$

Equating sine and cosine terms results in

$$\frac{\omega x_1}{U}\cos\phi_s - \sin\phi_s = -\left(\frac{\omega x_1}{U}\right)\left(\frac{x_2}{x_1}\right)\left(\frac{a_1}{a_2}\right) \tag{A13}$$

$$\cos\phi_s + \left(\frac{\omega x_1}{U}\right)\sin\phi_s = \left(\frac{a_1}{a_2}\right). \tag{A14}$$

Solving Eqs. (A13) and (A14) for $\sin\phi_s$ and $\cos\phi_s$ results in the following relationships:

$$\sin\phi_s = \frac{\dfrac{\omega x_1}{U}\left(1 + \dfrac{x_2}{x_1}\right)}{\left(\dfrac{a_2}{a_1}\right)\left[1 + \left(\dfrac{\omega x_1}{U}\right)^2\right]} \tag{A15}$$

$$\cos\phi_s = \frac{\dfrac{a_1}{a_2} - \dfrac{x_2}{x_1}\left(\dfrac{\omega x_1}{U}\right)^2}{1 + \left(\dfrac{\omega x_1}{U}\right)^2}. \tag{A16}$$

A boundary condition that must be satisfied is that $\sin\phi_s$ cannot be greater than one. Therefore,

$$\frac{\partial(\sin \phi_s)}{\partial\left(\frac{\omega x_1}{U}\right)} = 0 = \frac{\left(1 + \frac{x_2}{x_1}\right)\left[1 + \left(\frac{\omega x_1}{U}\right)^2 - 2\left(\frac{\omega x_1}{U}\right)^2\right]}{\left(\frac{a_2}{a_1}\right)\left[1 + \left(\frac{\omega x_1}{U}\right)^2\right]^2} . \tag{A17}$$

The value of $\omega x_1/U$ which satisfies Eq. (A17) is $\omega x_1/U = 1$. This result can be used to determine the relationship between the crank-length ratio and the strut-spacing ratio by substituting $\omega x_1/U = 1$ in Eq. (A15) as follows:

$$\sin \phi_s = 1 = \frac{\left(1 + \frac{x_2}{x_1}\right)}{2\left(\frac{a_2}{a_1}\right)} \tag{A18}$$

or, restating Eq. (A18),

$$\frac{a_2}{a_1} = \frac{1}{2}\left(1 + \frac{x_2}{x_1}\right) . \tag{A19}$$

The present Planar Motion Mechanism was designed having equal crank lengths. Therefore, in accordance with Eq. (A19), the strut spacing with respect to the body CG must be equal. For these conditions, the expression for the phase angle between struts for pure pitching motion reduces to

$$\cos \phi_s = \frac{1 - \left(\frac{\omega x}{U}\right)^2}{1 + \left(\frac{\omega x}{U}\right)^2} \tag{A20}$$

and the body pitch angle relation becomes

$$\theta = -\left(\frac{2a}{b} \sin \frac{\phi_s}{2}\right)\left[\cos\left(\omega t - \frac{\phi_s}{2}\right)\right] \tag{A21}$$

where

$$\left(\frac{2a}{b} \sin \frac{\phi_s}{2}\right)$$

is the maximum amplitude of the pitch angle θ_o.

As can be seen from Fig. 5, there is a given relationship between the point in the cycle when the pitch angle is zero and the zero point of the resolver (synchronous switch or sine-cosine potentiometer). The pitch angle trajectory of the model is a direct function of the phase angle between struts as shown by Eq. (A21). Therefore, the zero-pitch-angle point $(\omega t)_1$ will vary with strut-phase angle. This requires that the resolver be repositioned and synchronized with the zero-pitch-angle point for each condition of pure pitching.

The relationship between the zero-pitch-angle point $(\omega t)_1$ and the strut-phase angle can be determined from Eq. (A5). At the point $(\omega t)_1$ in the cycle, $\phi = 0$, $z_1 = z_2$, and z_o is a maximum. Therefore for $x_2/x_1 = a_2/a_1 = 1$, Eq. (A5) reduces to

$$\dot{z}_o = 0 = (1 + \cos \phi_s) \cos \omega t + \sin \phi_s \sin \omega t \tag{A22}$$

and

$$\tan \omega t = \frac{1 + \cos \phi_s}{\sin \phi_s} \tag{A23}$$

or

$$(\omega t) = \tan^{-1} \left[\frac{1 + \cos \phi_s}{\sin \phi_s} \right] . \tag{A24}$$

Differentiating with respect to ϕ_s yields

$$\frac{\partial(\omega t)}{\partial \phi_s} = \frac{1}{2} . \tag{A25}$$

APPENDIX B

Derivation of Reduction Equations

The Planar Motion Mechanism separates the motions of a body moving through a fluid into the hydrodynamically pure pitching and pure heaving motions as defined in Fig. 3. The differential equations of motion referred to a moving body axis system are used to establish a direct and explicit relationship between the various rotary and acceleration derivatives and the measured quadrature and in-phase components of the forces and moments. The linear force and moment equations describing the body motions with respect to the initial equilibrium conditions can be written as:

Transverse Force:

$$Y = Y_{\dot{r}} \dot{r} + \left(\frac{1}{2} \rho \ell^3 Y_r' + m\right) rU + (Y_{\dot{v}} - m)\dot{v}$$

$$+ \left(\frac{1}{2} \rho \ell^2 U Y_v'\right) v + \left(\frac{1}{2} \rho \ell^3 Y_p'\right) p + Y_{\dot{p}} \dot{p} . \tag{B1}$$

Normal Force:

$$Z = Z_{\dot{q}}\dot{q} + \left(\frac{1}{2}\rho\ell^3 Z_q' + m\right) qU + (Z_{\dot{w}} - m)\dot{w}$$
$$+ \left(\frac{1}{2}\rho\ell^2 UZ_w'\right) w + \left(\frac{1}{2}\rho\ell^2 UZ_v'\right) v + Z_* . \tag{B2}$$

Rolling Moment:

$$K = (K_{\dot{p}} - I_x)\dot{p} + \left(\frac{1}{2}\rho\ell^4 UK_p'\right) p + K_\phi + K_{\dot{r}}\dot{r}$$
$$+ \left(\frac{1}{2}\rho\ell^4 UK_r'\right) r + K_{\dot{v}}\dot{v} + \left(\frac{1}{2}\rho\ell^3 UK_v'\right) v . \tag{B3}$$

Pitching Moment:

$$M = (M_{\dot{q}} - I_y)\dot{q} + \left(\frac{1}{2}\rho\ell^4 UM_q'\right) q + M_\theta\theta + M_{\dot{w}}\dot{w}$$
$$+ \left(\frac{1}{2}\rho\ell^3 UM_w'\right) w + \left(\frac{1}{2}\rho\ell^3 UM_v'\right) v + M_* . \tag{B4}$$

Yawing Moment:

$$N = (N_{\dot{r}} - I_z)\dot{r} + \left(\frac{1}{2}\rho\ell^4 UN_r'\right) r + N_{\dot{v}}\dot{v}$$
$$+ \left(\frac{1}{2}\rho\ell^3 UN_v'\right) v + \left(\frac{1}{2}\rho\ell^4 UN_p'\right) p + N_{\dot{p}}\dot{p} . \tag{B5}$$

PURE HEAVING MOTION

The reduction equations for the pure heaving motion can be derived using Eqs. (A9), (B2), and (B4). For this motion, the pitch angle θ is zero at all times since the phase angle between the struts is zero.

As shown schematically in Figs. 3b and 4, the vertical displacement of the body CG can be expressed as

$$z_o = a \sin \omega t , \tag{B6}$$

the linear velocity as

$$\dot{z}_o = a\omega \cos \omega t , \tag{B7}$$

and the linear acceleration as

$$\ddot{z}_o = -a\omega^2 \sin \omega t . \tag{B8}$$

Since $\theta = q = \dot{q} = 0$, Eq. (A9) reduces to $\dot{z}_0 = w$. Therefore

$$w = a\omega \cos \omega t \tag{B9}$$

and

$$\dot{w} = -a\omega^2 \sin \omega t \, . \tag{B10}$$

Substituting Eqs. (B9) and (B10) in Eqs. (B2) and (B3), results in

$$Z = -a\omega^2(Z_{\dot{w}} - m_m) \sin \omega t + a\omega\left(\frac{1}{2}\,\rho \ell^2\; U Z_w{}'\right) \cos \omega t + Z_* \tag{B11}$$

and

$$M = -a\omega^2 M_{\dot{w}} \sin \omega t + a\omega\left(\frac{1}{2}\,\rho \ell^3 U M_w{}'\right) \cos \omega t + M_* \tag{B12}$$

where m_m is the model mass.

The component of force and moment in phase with the motion can be written as

$$Z_{in} = -a\omega^2(Z_{\dot{w}} - m) \tag{B13}$$

and

$$M_{in} = -a\omega^2 M_{\dot{w}} \, . \tag{B14}$$

The internal balance system, shown in Fig. 6, measures the components of force at two points spaced equidistant from the body CG. Therefore, Eqs. (B13) and (B14) can be rewritten as

$$(Z_1)_{in} + (Z_2)_{in} = -a\omega^2(Z_{\dot{w}} - m) \tag{B15}$$

and

$$x\left[(Z_2)_{in} - (Z_1)_{in}\right] = -a\omega^2 M_{\dot{w}} . \tag{B16}$$

The heaving acceleration derivatives, written in nondimensional form can be expressed as

$$(Z_{\dot{w}}{}' - m_m{}') = -\frac{\partial\left[(Z_1{}')_{in} + (Z_2{}')_{in}\right]}{\partial \dot{w}_o{}'} \tag{B17}$$

and

$$M_{\dot{w}}{}' = -\frac{x}{\ell}\,\frac{\partial\left[(Z_2{}')_{in} - (Z_1{}')_{in}\right]}{\partial \dot{w}_o{}'} \tag{B18}$$

where

$$\dot{w}_o' = \frac{a}{\ell}\,\frac{\omega^2\ell^2}{U^2}$$

is the amplitude of the linear acceleration.

Similarly, the reduction equations for the case of pure sideslipping (lateral translatory motion), as presented in Table 2, can be derived.

PURE PITCHING MOTION

The condition for pure pitching, as studied in Appendix A, is satisfied when the angle of attack α, measured at the CG, is equal to zero at all times. For this condition, the resultant linear velocity w and linear acceleration $\dot{w}$ are zero. The pitch angle, pitching velocity, and pitching acceleration can be expressed as

$$\theta = \frac{z_2 - z_1}{b} = -\left(\frac{2a}{b}\sin\frac{\phi_s}{2}\right)\left[\cos\left(\omega t - \frac{\phi_s}{2}\right)\right], \tag{B19}$$

the angular velocity as

$$\dot{\theta} = q = -\omega\left(\frac{2a}{b}\sin\frac{\phi_s}{2}\right)\left[-\sin\left(\omega t - \frac{\phi_s}{2}\right)\right], \tag{B20}$$

and the angular acceleration as

$$\ddot{\theta} = \dot{q} = \omega^2\left(\frac{2a}{b}\sin\frac{\phi_s}{2}\right)\left[\cos\left(\omega t - \frac{\phi_s}{2}\right)\right] \tag{B21}$$

where

$$\left(\frac{2a}{b}\sin\frac{\phi_s}{2}\right)$$

is the maximum amplitude of the pitch angle θ_o.

Substituting Eqs. (B19), (B20), and (B21) in Eqs. (B2) and (B4) yields:

$$\begin{aligned} Z = {} & \omega^2\left(\frac{2a}{b}\sin\frac{\phi_s}{2}\right) Z_{\dot{q}}\cos\left(\omega t - \frac{\phi_s}{2}\right) \\ & - \omega U\left(\frac{2a}{b}\sin\frac{\phi_s}{2}\right)\left(\frac{1}{2}\rho\ell^3 Z_q' + m_m\right)\left[-\sin\left(\omega t - \frac{\phi_s}{2}\right) + Z_*\right. \end{aligned} \tag{B22}$$

and

$$M = \omega^2 \left(\frac{2a}{b} \sin \frac{\phi_s}{2}\right) (M_{\dot{q}} - I_{ym}) \cos \left(\omega t - \frac{\phi_s}{2}\right)$$
$$- \omega U \left(\frac{2a}{b} \sin \frac{\phi_s}{2}\right) \left(\frac{1}{2} \rho \ell^4 M_q'\right) \left[- \sin \left(\omega t - \frac{\phi_s}{2}\right)\right]$$
$$- \left(\frac{2a}{b} \sin \frac{\phi_s}{2}\right) (M_\theta)_m \left[\cos \left(\omega t - \frac{\phi_s}{2}\right)\right] + M_* \tag{B23}$$

where I_{ym} and $(M_\theta)_m$ refer to the model moment of inertia and metacentric stability, respectively.

As for the heaving case, in-phase and quadrature components of force and moment can be written as:

$$(Z_1)_{in} + (Z_2)_{in} = \omega^2 \left(\frac{2a}{b} \sin \frac{\phi_s}{2}\right) Z_{\dot{q}} \tag{B24}$$

$$(Z_1)_{out} + (Z_2)_{out} = -\omega U \left(\frac{2a}{b} \sin \frac{\phi_s}{2}\right) \left(\frac{1}{2} \rho \ell^3 Z_q' + m_m\right) \tag{B25}$$

$$x\left[(Z_2)_{in} - (Z_1)_{in}\right] = \omega^2 \left(\frac{2a}{b} \sin \frac{\phi_s}{2}\right) (M_{\dot{q}} - I_{ym}) - M_{\theta m} \left(\frac{2a}{b} \sin \frac{\phi_s}{2}\right) \tag{B26}$$

$$x\left[(Z_2)_{out} - (Z_1)_{out}\right] = -\omega U \left(\frac{2a}{b} \sin \frac{\phi_s}{2}\right) \left(\frac{1}{2} \rho \ell^4 M_q'\right) \tag{B27}$$

The pitching rotary and acceleration derivatives, written in nondimensional form, can be expressed as:

$$Z_{\dot{q}}' = \frac{\partial\left[(Z_1')_{in} + (Z_2')_{in}\right]}{\partial \dot{q}_o'} \tag{B28}$$

$$(Z_q' + m_m') = -\frac{\partial\left[(Z_1')_{out} + (Z_2')_{out}\right]}{\partial q_o'} \tag{B29}$$

$$(M_q' - I_{ym}') = \frac{x}{\ell} \frac{\left[(Z_2')_{in} - (Z_1')_{in}\right]}{\partial \dot{q}_o'} + \frac{\dfrac{(M_\theta)_m}{\frac{1}{2}\rho \ell^2}}{\omega^2} \tag{B30}$$

$$M_q' = -\frac{x}{\ell}\,\frac{\partial\left[(Z_2')_{out} - (Z_1')_{out}\right]}{\partial q_o'} \tag{B31}$$

where

$$q_o' = \left(\frac{2a}{b}\sin\frac{\phi_s}{2}\right)\frac{\omega\ell}{U} \tag{B32}$$

and

$$\dot{q}_o' = \left(\frac{2a}{b}\sin\frac{\phi_s}{2}\right)\frac{\omega^2\ell^2}{U^2} \tag{B33}$$

are the maximum amplitudes of the angular velocity and acceleration, respectively.

The relationships for pure yawing and rolling, presented in Table 2, can be derived in a similar manner.

The model mass m_m and metacentric stability $(M_\theta)_m$ are evaluated experimentally by performing inclining tests (standstills). The model moment of inertia I_{ym} is determined from oscillation tests performed in air. For these tests, the model-ballast condition is the same as during the regular tests.

APPENDIX C

Mathematical Operations Performed by Instrumentation System

As indicated in the section entitled "Instrumentation for Static and Dynamic Stability Tests," the operation of the present electronic system differs from that described in Ref. 2 in that a true integration of the gage signal is performed.

To illustrate, assume a pure heaving condition which results in a gage signal of the form such as given in Fig. 4:

$$Z_R = Z_* + Z_o \sin(\omega t - \phi) \tag{C1}$$

which can be written as

$$Z_R = Z_* + Z_o(\cos\phi)\sin\omega t - Z_o(\sin\phi)\cos\omega t \tag{C2}$$

or

$$Z_R = Z_* + Z_{in}\sin\omega t - Z_{out}\cos\omega t. \tag{C3}$$

The in-phase and quadrature (out-of-phase) components can be obtained by operating on the gage signal in the following manner:

$$Z_{in} = \frac{1}{\pi}\int_0^{2\pi} Z_R \sin \omega t \; d(\omega t) \tag{C4}$$

and

$$Z_{out} = \frac{1}{\pi}\int_0^{2\pi} Z_R \cos \omega t \; d(\omega t). \tag{C5}$$

The operations indicated by Eqs. (C4) and (C5) are performed by the force-component separator, sine-cosine potentiometer, integrating amplifier, and timer diagrammed in Fig. 22.

The result of the integration is provided by the digital readout and is defined as

$$Z_{in} = Z_o \cos \phi \tag{C6}$$

and

$$Z_{out} = -Z_o \sin \phi. \tag{C7}$$

Likewise, for the pure pitching condition the resultant gage signal has the form (see Fig. 5)

$$Z_R = Z_* + Z_o \cos \left[\left(\omega t - \frac{\phi_s}{2}\right) - \phi\right] \tag{C8}$$

or

$$Z_R = Z_* + (Z_o \cos \phi) \cos \left(\omega t - \frac{\phi_s}{2}\right) + (Z_o \sin \phi) \sin \left(\omega t - \frac{\phi_s}{2}\right). \tag{C9}$$

The integration performed is as follows:

$$Z_{in} = \frac{1}{\pi}\int_{(\omega t)_1}^{(\omega t)_1 + 2\pi} Z_R \sin \left[\omega t - (\omega t)_1\right] \; d(\omega t) \tag{C10}$$

and

$$Z_{out} = \frac{1}{\pi}\int_{(\omega t)_1}^{(\omega t)_1 + 2\pi} Z_R \cos \left[\omega t - (\omega t)_1\right] \; d(\omega t) \tag{C11}$$

where

$$(\omega t)_1 = \frac{\pi}{2} + \frac{\phi_s}{2} .$$

Equations (C10) and (C11) reduce to

$$Z_{in} = -Z_o \cos \phi \tag{C12}$$

and

$$Z_{out} = Z_o \sin \phi . \tag{C13}$$

Thus, the operation performed by the electronic system is equivalent to determining the Fourier coefficients of the fundamental of the gage signal.

APPENDIX D

Equations of Motion for Submarines

The differential equations of motion in dimensional form, referred to a moving body axes system which is coincident with the principal axes of inertia and having the origin at the center of mass, can be written for the case when the submarine is initially in level flight and at a steady forward speed as:

Axial Force

$$
\begin{aligned}
m(\dot{u} - vr + wq) = {} & \frac{\rho}{2}\ell^3 \left[X'_{\dot{u}}\dot{u} - Y'_{\dot{v}}vr + Z'_{\dot{w}}wq\right] \\
& + \frac{\rho}{2}\ell^2 \left[X'_{(uu)}u^2 + X'_{(vv)}v^2 + X'_{(ww)}w^2\right] \\
& + \frac{\rho}{2}\ell^2 u^2 \left[X'_{(\delta r \delta r)}\delta_r^{\,2} + X'_{(\delta s \delta s)}\delta_s^{\,2} + X'_{(\delta b \delta b)}\delta_b^{\,2}\right] \\
& + (F_x)_p .
\end{aligned}
$$

Lateral Force

$$
\begin{aligned}
m(\dot{v} - wp + ur) = {} & \frac{\rho}{2}\ell^3 \left[Y'_{\dot{v}}\dot{v} - Z'_{\dot{w}}wp\right] \\
& + \frac{\rho}{2}\ell^2 \left[Y'_{*}u^2 + Y'_{v}uv + Y'_{(v|v|)}v|v|\right] \\
& + \frac{\rho}{2}\ell^3 \left[Y'_{r}ur + Y'_{(|r|\delta r)}u|r|\delta r + Y'_{(|v|r)}|v|r + Y'_{p}up\right] \\
& + \frac{\rho}{2}\ell^4 \left[Y'_{\dot{r}}\dot{r} + Y'_{\dot{p}}\dot{p}\right] + \frac{\rho}{2}\ell^2 u^2\, Y'_{\delta r}\delta_r + (F_y)_s .
\end{aligned}
$$

Normal Force

$$m(\dot{w} - uq + vp) = \frac{\rho}{2}\ell^3\left[Z'_{\dot{w}}\dot{w} + Y'_{\dot{v}}vp\right]$$

$$+ \frac{\rho}{2}\ell^2\left[Z'_{*}u^2 + Z'_{w}uw + Z'_{(w|w|)}w|w|\right]$$

$$+ \frac{\rho}{2}\ell^3\left[Z'_{q}uq + Z'_{(|q|\delta s)}u|q|\delta s + Z'_{(|w|q)}|w|q\right]$$

$$+ \frac{\rho}{2}\ell^2 Z'_{(vv)}v^2 + \frac{\rho}{2}\ell^3 Z'_{(vr)}vr + \frac{\rho}{2}\ell^4 Z'_{(rr)}r^2$$

$$+ \frac{\rho}{2}\ell^2u^2\left[Z'_{\delta s}\delta_s + Z'_{\delta b}\delta_b\right] + \frac{\rho}{2}\ell^4 Z'_{\dot{q}}\dot{q} + (F_z)_s.$$

Rolling Moment

$$I_x\dot{p} + (I_z - I_y)qr = \frac{\rho}{2}\ell^5\left[K'_{\dot{p}}\dot{p} + (N'_{\dot{r}} - M'_{\dot{q}})qr + K'_{\dot{r}}\dot{r} + K_{(p|p|)}p|p|\right]$$

$$+ \frac{\rho}{2}\ell^3\left[K'_{*}u^2 + K'_{v}uv + K'_{(v|v|)}v|v|\right]$$

$$+ \frac{\rho}{2}\ell^4\left[K'_{p}up + K'_{r}ur + K'_{\dot{v}}\dot{v}\right]$$

$$+ \frac{\rho}{2}\ell^3 u^2 K'_{\delta r}\delta_r + Bz_B \sin\phi + (Q_x)_s.$$

Pitching Moment

$$I_y\dot{q} + (I_x - I_z)rp = \frac{\rho}{2}\ell^5\left[M'_{\dot{q}}q + (K'_{\dot{p}} - N'_{\dot{r}})rp\right]$$

$$+ \frac{\rho}{2}\ell^3\left[M'_{*}u^2 + M'_{w}uw + M'_{(w|w|)}w|w|\right]$$

$$+ \frac{\rho}{2}\ell^4\left[M'_{q}uq + M'_{(|q|\delta s)}u|q|\delta s + M'_{(|w|q)}|w|q\right]$$

$$+ \frac{\rho}{2}\ell^3 M'_{(vv)}v^2 + \frac{\rho}{2}\ell^4 M'_{(vr)}vr$$

$$+ \frac{\rho}{2}\ell^5 M'_{(rr)}r^2 + \frac{\rho}{2}\ell^4 M'_{\dot{w}} + \frac{\rho}{2}\ell^3u^2\left[M'_{\delta s}\delta_s + M'_{\delta b}\delta_b\right]$$

$$+ Bz_B \sin\theta + (Q_y)_s$$

Yaying Moment

$$I_z\dot{r} + (I_y - I_x)pq = \frac{\rho}{2}\ell^5\left[N'_{\dot{r}}\dot{r} + (M'_{\dot{q}} - K'_{\dot{p}})pq + N'_{\dot{p}}\dot{p}\right]$$

$$+ \frac{\rho}{2}\ell^3\left[N'_*u^2 + N'_v uv + N'_{(v|v|)}v|v|\right]$$

$$+ \frac{\rho}{2}\ell^4\left[N'_r ur + N_{(|r|\delta r)}u|r|\delta r + N'_{(|v|r)}|v|r\right]$$

$$+ \frac{\rho}{2}\ell^4\left[N'_p up + N'_{\dot{v}}\dot{v}\right] + \frac{\rho}{2}\ell^3 u^2 N'_{\delta r}\delta_r + (Q_z)_s.$$

Kinematic Relations

$$U^2 = u^2 + v^2 + w^2$$

$$\dot{z}_I = -u\sin\theta + v\cos\theta\sin\phi + w\cos\theta\cos\phi$$

$$\cong w - u\theta + v\phi$$

$$\dot{\phi} = p + \dot{\psi}\sin\theta$$

$$\cong p + r\theta$$

$$\dot{\theta} = \frac{q - \dot{\psi}\cos\theta\sin\phi}{\cos\phi}$$

$$\cong q - r\phi$$

$$\dot{\psi} = \frac{r + \dot{\theta}\sin\phi}{\cos\theta\cos\phi}$$

$$\cong r + q\phi.$$

Auxiliary Relations

$$(F_x)_P = a_1u^2 + a_2uU_c + a_3U_c^2$$

or

$$= (1-t)\,aU_c^2.$$

DISCUSSION

H. N. Abramson (Southwest Research Institute, San Antonio)

Submerged body technology shows two interesting trends; one is toward increasing fineness and the other is toward higher speed. These two together tend to introduce a new important factor and this is the elasticity of the structure. In short, hydroelastic considerations may become important for stability and control investigations of submerged bodies. I would very much like to have the author's comments on what considerations he and his colleagues have given to introducing hydroelastic effects into their theoretical and experimental studies.

E. C. Tupper (Admiralty Experiment Works)

The author mentioned in his paper the question of certain standards by which the performance of the submarine could be judged. I would like the author if he will, to state what these standards are in both the vertical and the horizontal plane. Only by studying in a computer, say, the way in which the performance of the submarine varies as regards these standards, can one judge the importance of various hydrodynamic derivatives. For instance, the author mentioned that we have what are commonly called the static, rotary, and acceleration derivatives. We feel, at the Admiralty Experiment Works, that the acceleration derivatives are not critical. There are basically four for the simple equations of motion in the vertical plane and we feel that two of these can be ignored and the other two can be calculated with sufficient accuracy and therefore do not need to be measured.

We have not studied the horizontal plane problem completely, but we feel that the most important point here is the nonlinearity introduced by the very large reductions in speed which can occur when maneuvering in the horizontal plane. I would like to make a plea, therefore, for some description of the standards which the author considers to be important.

It would be very interesting if the author could give us any information on comparisons between results with the oscillator technique which he has described and other methods of test, in particular the comparison with the rotary derivatives between the oscillator and rotating arm methods of testing.

S. T. Mathews (National Research Council, Ottawa)

I think we should congratulate Mr. Goodman and his colleagues at the David Taylor Model Basin for developing what I consider the most powerful method of considering this submarine stability and control problem, experimentally anyway. Surely these experimental results are most useful or even essential before we further develop the theoretical methods. I have a few points of detail. I would like to ask Mr. Goodman if the carrying out of static moment and force tests is not superfluous, because the same results are obtained by the oscillating heaving tests. I would be glad to have any comments he has on how the results obtained by the two methods compare. Mr. Tupper took one of my points. I was going to ask specifically if we could have any comparisons between results obtained for the rotary static moment and force derivations from the oscillating mechanism as compared with a rotating arm. It seems to me that no mention has been made of surface models; for linear seaworthiness considerations one could obtain much useful data using the oscillating mechanism technique, in pitch and heave, and also we could get results in yaw, I would think, certainly at low

Froude numbers. It would also seem that the technique could be extended to cover nonlinearities if a different sort of recording technique were used.

J. P. Breslin (Davidson Laboratory, Stevens Institute of Technology)

I have a few questions I would like to put to the author and the first one is the question as to what the David Taylor Model Basin does about strut interference on the planar motion experiments.

The Davidson Laboratory has been operating a rotating arm now for about 16 years and has been greatly interested in refining and improving the techniques, particularly for the investigation of interferences, of coupling effects, and of nonlinear behavior of submarines and bodies of revolution with a mind to exploring the behavior of such vessels in radical maneuvers. In this regard, it is rather interesting that in the model regime the Navy has been able to get along without very much information in this area of large course deviations for this long period of time. We look forward with great interest to the developments which will come from the David Taylor rotating arm, not only for the comparisons for which Mr. Tupper asked, but also for the predictions of nonlinear coefficients which are necessary for modern-day treatment of evasive and radical maneuvers.

My second point has to do with the assertion that in regard to accuracy one ought to look somewhat askance at rotating arm methods for determining static derivatives. The Davidson Laboratory and the Model Basin have had a number of discussions on this matter and as a matter of fact the Model Basin has supported us in the very recent past in an experimental investigation in which we conducted experiments in the straight tank to measure static derivatives and repeated the experiments on the rotating arm, interpolating or extrapolating, depending upon how you interpret the procedure to obtain the derivatives at infinite radius. I am happy to say that these experiments,* as well as several that have been made in the past, always give very close agreement. Of course, general statements of a sweeping nature are all subject to exceptions and perhaps the class of bodies with very small damping is one in which close scrutiny should be made of the difference between the techniques.

Finally, I would like to call the attention of the participants to the great usefulness of the small model in such explorations to map out the gross effects of shape and control surface location so that modern concepts of optimizing maneuverability and controllability can be more readily achieved. The David Taylor Model Basin has certainly done an exceptional job in developing equipment which is suitable for proof testing of designs and this is a very important aspect of their part in the naval establishment, but it is urged that the use of the rotating arm at the Davidson Laboratory and other small facilities be continued for interesting exploratory research.

R. Brard (Bassin d'Essais des Carênes, Paris)

I would like to say how we appreciate the work done by the David Taylor Model Basin in order to study the maneuverability of the submarines and I would too address warm congratulations to the staff, and particularly Mr. Goodman, for their beautiful results, specially those concerning the maneuvering of the submarine under the polar ice cap.

*S. Tsakonas, "Effect of Appendage and Hull Form on Hydrodynamic Coefficients of Surface Ships," Davidson Laboratory Report 740, July 1959

I would ask him if he has given reflexion to the following point. If the motion of the ship is not steady, the hydrodynamic forces and moments on the ship depend, partly, at the instant *t*, on the motion of the ship before this instant *t*. Therefore, the equations of the motion of the ship are not exactly the same as in the case where the forces and moments would at each instant equal their values in steady motion. One study made in France shows that the condition of stability is not modified; but the trend to the steady motion is more accentuated. Thus, the transient motions are affected in such a manner that, furthermore, seems to be favorable.

Alex Goodman

Dr. Todd's paper raised a question pertaining to the stability and control requirements of a large submarine tanker. In my opinion, it would seem that such a vehicle would require a high degree of inherent stability as well as a properly designed autopilot. I noted a touch of pessimism in Mr. Newton's comment on Dr. Todd's paper which I cannot share. I think that with the techniques and means available today, solutions to the stability and control problems of such vehicles can be obtained without any difficulty.

I would like to thank the discussers for their comments. I will be brief with my replies to the various questions that have been asked. Dr. Abramson asked whether the effects of hydroelasticity on the stability and control of submarines have been considered. We have not considered such effects. However, prediction of full-scale performance based on rigid-body dynamics has been very good. Answers to several of Mr. Tupper's questions are in the written manuscript as well as in other Model Basin sources. Mr. Tupper questioned the need for the experimental determination of the acceleration derivatives by stating that theoretical techniques are available to estimate these derivatives. It is true that theoretical means are available for estimating the acceleration derivatives; however, in my opinion they are not accurate enough when it is required to determine the degree of stability. I can only say that by using the results obtained from tests using the Planar-Motion-Mechanism System we have been able to achieve excellent correlation with full scale performance. Correlations between this technique and the rotating arm technique are planned using the same model, essentially the same support system, and the same force-measuring-instrumentation system. I would like to thank Mr. Mathews for his compliments. As far as his question pertaining to the use of the Planar Motion Mechanism for the surface ship model testing, I can only say that some thought has been given to using this technique for such problems. However, I think we will first obtain some experience using the rotating-arm technique for the surface ship problem. Dr. Breslin raised a question regarding the effects of strut interference on the measurement. An extensive and detailed study of strut interference has been conducted at the Model Basin. The results of this study led to the strut design which has been incorporated in the Planar-Motion-Mechanism System, that is, small-chord struts in the vicinity of the model and angles of attack of the body being taken in the plane of the strut. As I mentioned in my presentation, this eliminates the mutual interference effects between the strut and the body. There are small blockage effects. However, by choosing the proper extension of the lower half of the strut the resistance of bodies can be measured as accurately as is done by other standard techniques. As to the required accuracy of static coefficients, I don't recall to which paper Dr. Breslin was referring, but the one I remember which shows the comparison between static coefficients, obtained from straight line tests and those obtained by the extrapolation technique differed by as much as 10 to 20 percent. This is not a small percentage when we are talking about performing accurate analyses of maneuvers. With regard to Dr. Breslin's comment as to the economy regarding small models compared to large models, this is an argumentative point. DTMB is at an advantage, since we feel that the large model is much cheaper to construct than a small specialized model. We use standard internal equipment which can be used from model to model, thereby eliminating the need for special purpose equipment for each model. There are other advantages associated with size. DTMB is not only in the business of checking specific designs; extensive systematic studies are also conducted at DTMB and the Planar-Motion-Mechanism System is very amenable to such studies and relatively cheap to operate. For example, it takes approximately one week of testing to completely define all the hydrodynamic characteristics for a specific submarine design.

* * *